

Cite this: *Chem. Sci.*, 2021, **12**, 1964

All publication charges for this article have been paid for by the Royal Society of Chemistry

Received 3rd August 2020  
Accepted 9th September 2020

DOI: 10.1039/d0sc04238b  
[rsc.li/chemical-science](http://rsc.li/chemical-science)

## 1. Introduction

Transition metal catalysts have become widely adopted as useful tools in modern synthetic organic chemistry because of their diverse reactivity in enabling various molecular transformations. The chemistry has expansively grown along with the development of supporting ligands, which significantly affect the reactivity and stability of the metal complexes in the primary coordination sphere. Various organic compounds such as phosphines, amines, ethers, and carbenes are employed as

<sup>a</sup>Department of Chemistry, Tokyo Institute of Technology, Ookayama, Meguro-ku, Tokyo 152-8551, Japan. E-mail: takayajun@chem.titech.ac.jp

<sup>b</sup>JST, PRESTO, Honcho, Kawaguchi, Saitama, 332-0012, Japan



*Jun Takaya received his PhD from Tokyo Institute of Technology (2004) under the supervision of Prof. Nobuharu Iwasawa. He joined Prof. John Hartwig at Yale University as a postdoctoral researcher in 2004. He was appointed as Assistant Professor at Tokyo Institute of Technology in 2005, and promoted to Associate Professor in 2014. He is also working as a PRESTO researcher of JST from 2017. He received*

*Incentive Award in Synthetic Organic Chemistry (2013), Merck-Banyu Lectureship Award (2014), and The Young Scientist's Prize (2016). His research interests include the development and catalytic application of new transition metal complexes.*

# Catalysis using transition metal complexes featuring main group metal and metalloid compounds as supporting ligands

Jun Takaya <sup>\*ab</sup>

Recent development in catalytic application of transition metal complexes having an M–E bond (E = main group metal or metalloid element), which is stabilized by a multidentate ligand, is summarized. Main group metal and metalloid supporting ligands furnish unusual electronic and steric environments and molecular functions to transition metals, which are not easily available with standard organic supporting ligands such as phosphines and amines. These characteristics often realize remarkable catalytic activity, unique product selectivity, and new molecular transformations. This perspective demonstrates the promising utility of main group metal and metalloid compounds as a new class of supporting ligands for transition metal catalysts in synthetic chemistry.

supporting ligands for p-block organic elements in the periodic table.<sup>1</sup> As a representative example, *N*-heterocyclic carbenes (NHCs) have been utilized as strong  $\sigma$ -donor ligands for various transition metals since the appearance of an isolable NHC in 1991,<sup>2a</sup> realizing highly efficient catalysis and sometimes enabling new molecular transformations.<sup>2b–d</sup> Development of new supporting ligands that supply unusual electronic and steric environments and molecular functions to transition metals has been an important challenge in expanding the chemistry of transition metal catalysts.

Recently, main group metal and metalloid compounds have emerged as a new class of supporting ligands for transition metals. These compounds often display characteristic coordination behaviour and electronic properties originating from their Lewis acidity and low electronegativity, which are usually not available with standard organic ligands. The redox activity and cooperative reactivity of these compounds are also of great interest. They are highly promising for exploring the new reactivity of transition metal catalysts for efficient molecular transformations. However, an M–E bond between a transition metal (M) and a main group metal or metalloid element (E) is usually unstable and not necessarily easy to form regardless of whether it is a covalent bond or a coordination bond. Therefore, development of new M–E complexes that are easily accessible and furnish sufficient stability and unique catalysis is highly desirable.

A useful strategy is to utilize rationally designed multidentate ligands as scaffolds for the M–E bonds (Fig. 1). A main group metal or metalloid element E is pre-incorporated into an organic ligand ( $X_mL_n$ ) to form a multidentate ligand containing an E atom as one of the components of coordinating moieties. Following complexation with a transition metal an M–E complex is afforded through coordination of E to M or oxidative addition of a bond between E and its anionic ligand to M (Fig. 1, route a). As another approach,



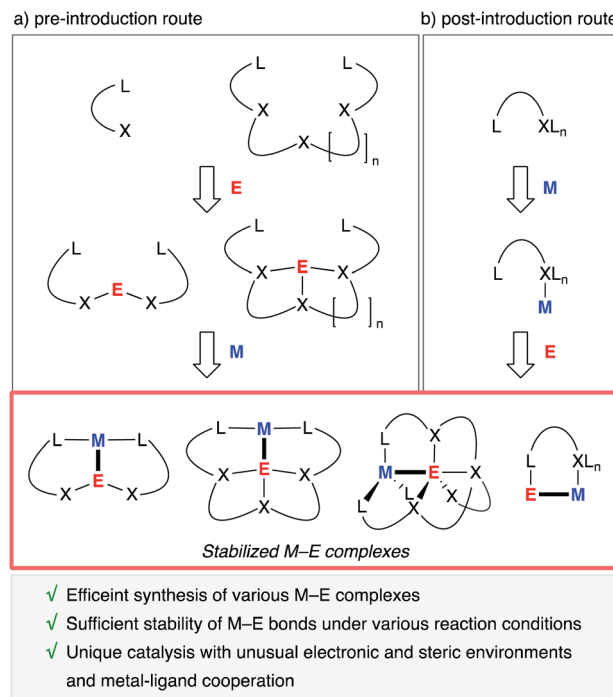


Fig. 1 Synthesis and catalytic application of stabilized M–E complexes.

post-introduction of a main group metal or metalloid element E to a transition metal complex M bearing a rationally designed pendant moiety to coordinate to E is also possible (route b). These strategies enable efficient synthesis of a variety of M–E complexes, which are stable enough to be utilized as catalysts under various reaction conditions.

This perspective article summarizes recent development of transition metal complexes having an M–E bond (E = main group metal or metalloid element), which is stabilized by a multidentate ligand, with an emphasis on catalysis where the main group metal or metalloid supporting ligand plays a crucial role in controlling the reactivity of the transition metal. E covers p-block metal and metalloid elements (B, Al, Ga, In, Si, Ge, Sb, and Bi) and a group 12 metal (Zn). We focus on the catalytic reactivity of M–E complexes employing E-containing tri- or tetradeятate ligand structures ( $L_2E$ - or  $L_3E$ -type ligands), in which the direct interaction of the E-ligand with M certainly occurs in catalysts or catalytically relevant intermediates. Examples where the E-ligand acts as a Lewis acidic pendant moiety for activation of substrates in the secondary coordination sphere are not included. They are often seen with rather flexible E-containing bidentate ligands.<sup>3</sup>

## 2. How does E act as a supporting ligand? – general classification of the functions

### 2.1 Acting as a $\sigma$ -acceptor ligand (Z-type ligand)

Lewis acidic metal and metalloid elements act as  $\sigma$ -acceptor ligands (Z-type ligand) *via* dative bonding with transition metals

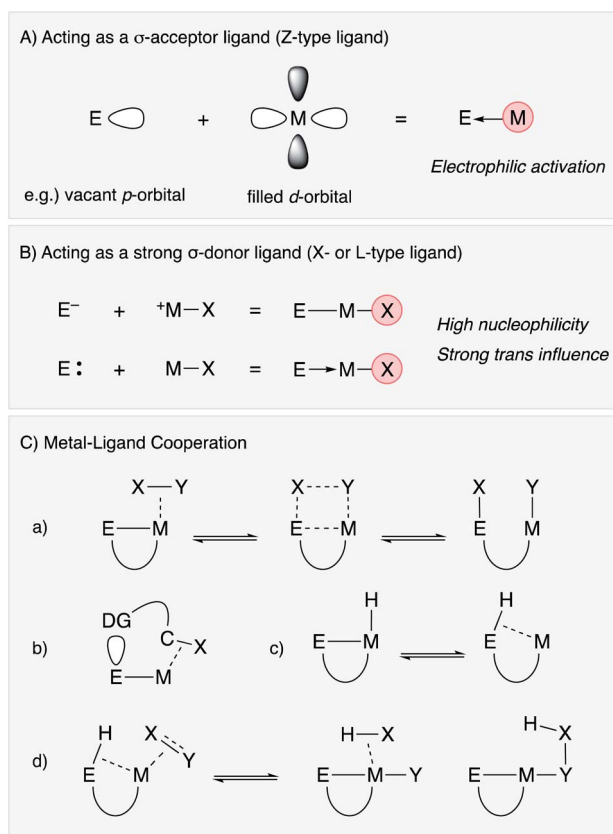


Fig. 2 General classification of the functions of M–E bonds.

(Fig. 2A).<sup>4,5</sup> This is often observed in group 13 element supporting ligands having a vacant p-orbital.<sup>3,6</sup> Lewis acidic group 12 metals and some of the electronically positive heavier group 14 and 15 compounds can also be  $\sigma$ -acceptors for transition metals.<sup>7–9</sup> The Z-type coordination activates the transition metal electrophilically by withdrawing electron density from the filled d-orbital, sometimes leading to change of the oxidation state of the transition metal not only in terms of formal description but also in terms of redox properties and reactivity. This is one of the characteristic properties of metal and metalloid supporting ligands distinct from standard organic ligands such as phosphines and amines, which usually coordinate to transition metals mainly through  $\sigma$ -donation along with partial  $\pi$ -back donation. Furthermore, the catalytic reactivity is modulative by exploiting the coordination and redox reactivity of the E-ligand. In particular, these characteristics are highly beneficial for electrophilic activation reactions of organic substrates such as alkynes and small molecules such as dihydrogen.

### 2.2 Acting as a strong $\sigma$ -donor ligand (X- or L-type ligand)

There are several examples of the X-type ligation of anionic group 13 and 14 atoms such as boron and silicon to transition metals to form covalent M–E bonds (Fig. 2B).<sup>10–14</sup> These metal and metalloid ligands act as strong  $\sigma$ -donors and often exhibit strong *trans* influence, which destabilizes the M–X bond at the *trans* position.<sup>15,16</sup> These characteristics lead to generation of

highly reactive transition metal catalysts for various bond activation and nucleophilic addition reactions. Furthermore, metallylenes, which are neutral, low valent group 13 or 14 element compounds having +1 or +2 oxidation states, respectively, have also been utilized as L-type supporting ligands for transition metals.<sup>17–22</sup> These metallylenes also act as strong  $\sigma$ -donors to facilitate various molecular transformations.

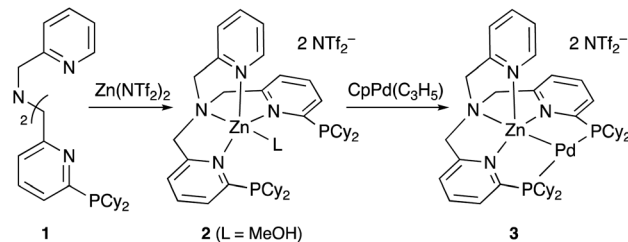
### 2.3 Metal-ligand cooperation (MLC)

In addition to the unique electronic characteristics described above, cooperative molecular activation and transformation are often enabled with M–E bonds through a kind of metal–ligand cooperation (MLC).<sup>23</sup> As a representative example, an M–B complex having a Z-type boron–ligand cooperatively activates a substrate X–Y such as dihydrogen with a vacant p-orbital on B, promoting unusual oxidative addition of the X–Y bond across the M–B bond (Fig. 2C(a)).<sup>7</sup> Similar MLC for activation of dihydrogen can also be considered with X-type boryl and aluminyl ligands, and they are successfully applied to various hydrogenation reactions. Moreover, the site-selective C–H bond activation of coordinated Lewis basic substrates such as pyridines is also considered as another type of MLC using the Lewis acidity of the E-ligand (Fig. 2C(b)). An M–E bond with an X-type heavier group 14 ligand, in particular a silyl ligand, undergoes facile interconversion between an  $\eta^2$ -(Si–H)M complex and an Si–M–H complex through reversible reductive elimination/oxidative addition of the Si–H bond due to its high reactivity (Fig. 2C(c)).<sup>13,14</sup> This is often involved in several catalytic cycles to generate coordinatively unsaturated metal species for substrate activation and transformations. Furthermore, unusual  $\sigma$ -bond metathesis reactions and metallation/elimination reactions that directly proceed between an  $\eta^2$ -(Si–H)M complex and substrates without formation of a metal hydride intermediate have also been reported accompanied by formation/dissociation of the silyl ligand (Fig. 2C(d)). These processes can be regarded as a kind of  $\sigma$ -bond assisted metathesis ( $\sigma$ -CAM),<sup>24</sup> which is distinct from usual oxidative addition/reductive elimination reactions or  $\sigma$ -bond metathesis reactions, demonstrating the privileged reactivity of M–E complexes.

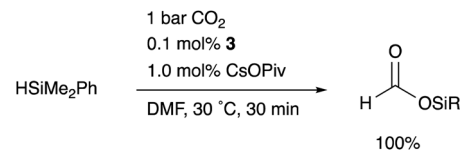
## 3. Catalysis using M–E complexes in synthetic reactions

### 3.1 Group 12 (E = Zn)

Although there are several reports on the synthesis and stoichiometric reactivity of M–E complexes with group 12 ligands (E = Zn, Cd, and Hg), their catalytic applications have scarcely been investigated to date.<sup>25</sup> Tauchert reported the synthesis of a Pd complex **3** having Zn as a supporting ligand (a Zn-metalloligand) by utilizing a tris(pyridylmethyl)amine derivative **1** bearing two phosphine side arms as a scaffold for the Pd–Zn bond (Scheme 1).<sup>26</sup> Pre-introduction of Zn(NTf<sub>2</sub>) into **1** afforded the Zn-metalloligand **2**, which reacted with CpPd(C<sub>3</sub>H<sub>5</sub>) to form a Pd–Zn bond. Theoretical calculations indicated that the Zn-metalloligand acts as a Z-type ligand for Pd *via* an



Scheme 1 Synthesis of the Pd–Zn complex **3**.



Scheme 2 Hydrosilylation of CO<sub>2</sub> catalyzed by the Pd–Zn complex **3**.

acceptor s-orbital, which is a relatively weak acceptor compared with empty p-orbitals of group 13 elements such as B and Al. Corresponding Pd–Cu and Pd–Li complexes were also synthesized similarly, and the magnitude of  $\sigma$ -accepting ability was clarified to be in the order of Zn > Cu > Li. The Pd–Zn complex **3** exhibited high catalytic activity for hydrosilylation of CO<sub>2</sub> to give silyl formate (Scheme 2). A corresponding Pd complex without the Zn-metalloligand and Pd–Cu and Pd–Li complexes resulted in low catalytic activity, thus demonstrating the importance of the Zn-metalloligand for efficient catalysis.

### 3.2 Group 13 (E = B, Al, Ga, and In)

A lot of rationally designed B-containing tri- or tetridentate ligands have been developed to date, and selected examples are listed in Fig. 3.<sup>3,5,6</sup> These multidentate B-ligands are usually isolable and storable, enabling efficient synthesis of various M–B complexes by reacting with suitable transition metal precursors. These complexes display the unusual electronic nature and stoichiometric cooperative reactivity of the M–B bond for activation of substrates such as dihydrogen. Regarding catalytic applications, several reports briefly mentioned their catalytic activity for hydrogenation *etc.* although the role of the B-ligands is not necessarily clarified and advantageous.<sup>27</sup>

**3.2.1 Z-type borane ligand.** Important examples demonstrating the privileged reactivity of the M–B bond in catalysis have been reported using an *o*-phosphinophenyl linkage as a scaffold for the M–B bond. Bourissou developed bis- and tris(*o*-phosphinophenyl)boron **10** and **11** as boron-containing multidentate ligands and realized efficient syntheses and structural analyses of various transition metal complexes with them.<sup>28</sup> The boron atom in **10** and **11** usually acts as a  $\sigma$ -accepting Z-type ligand with its vacant p-orbital, which is fixed proximally to the metal center due to the rigid tri- or tetridentate structure. This Z-type ligation leads to efficient stabilization of an electron-rich metal center and generation of a highly electrophilic metal center. Cooperative activation of substrates *via* MLC of the M–B bond is also possible.



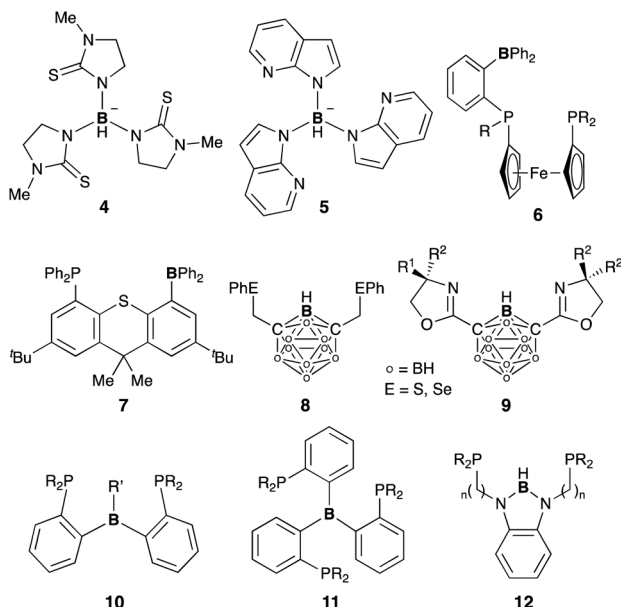
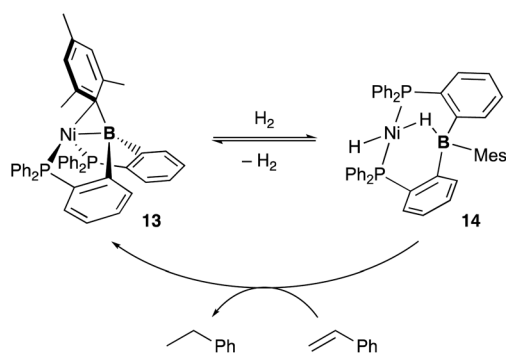
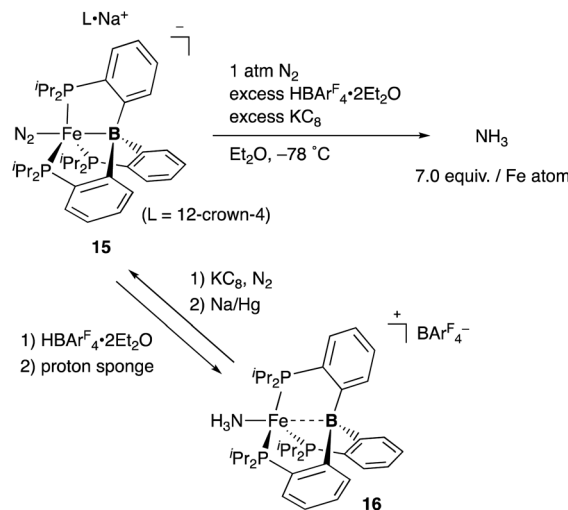


Fig. 3 Representative B-containing tri- or tetradentate ligands for M-B complexes.

Several catalytic reactions where the PBP-ligand **10** functions as a Z-type ligand and exhibits MLC have been reported. Peters developed a Ni complex **13** with the PBP-ligand, in which the Ni coordinates to the B-Mes moiety in an  $\eta^2$ -B,C fashion (Scheme 3).<sup>29</sup> The high catalytic activity of **13** for hydrogenation of alkenes was demonstrated under 1 atm of  $\text{H}_2$ . As a part of a plausible reaction mechanism, reversible oxidative addition of  $\text{H}_2$  across the Ni-B bond of **13** was evidenced by formation and structural characterization of a borohydride–hydride Ni complex **14**.<sup>30</sup> The Ni-B bond functioned as a kind of a frustrated Lewis pair for the heterolytic activation of  $\text{H}_2$ , where the Lewis acidic boron atom accepted  $\text{H}^-$  and the Lewis basic Ni accepted  $\text{H}^+$ . The details of the reaction mechanism and the electronic process for the activation of the H–H bond across the Ni-B bond are investigated theoretically, clarifying that the B atom assists in the H–H  $\sigma$ -bond activation *via* charge transfer from  $\text{H}_2$  to the Ni-B bond and stabilizes the Ni–H–B bridging structure.<sup>31</sup> A similar cooperative activation of the Si–H bond of



Scheme 3 Catalytic hydrogenation of alkenes via H–H  $\sigma$ -bond activation across the Ni-B bond of the PBP–Ni complex **13**.

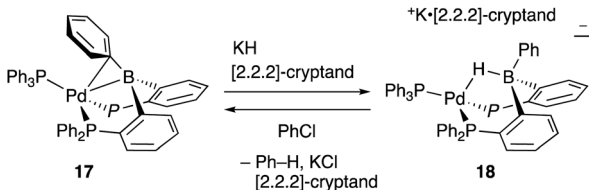


Scheme 4 Generation of ammonia from  $\text{N}_2$  catalyzed by the  $\text{P}_3\text{B}$ –Fe complex **15**.

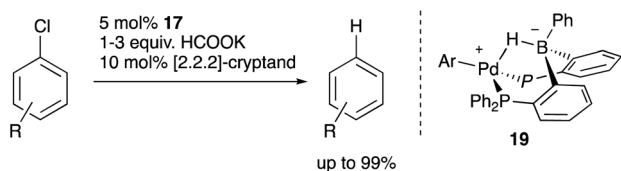
$\text{H}_2\text{SiPh}_2$  was also reported with the Ni–B complex **13**, realizing an efficient catalytic hydrosilylation reaction of aldehydes to obtain silyl ethers.<sup>32</sup>

Peters also demonstrated the high utility of the  $\text{P}_3\text{B}$ -ligand **11**, tris(*o*-phosphinophenyl)boron, to stabilize electron rich, low valent Fe complexes for the catalytic conversion of dinitrogen to ammonia (Scheme 4). An anionic  $\text{N}_2$ -coordinated Fe complex **15** was successfully prepared and structurally characterized by utilizing the  $\text{P}_3\text{B}$ -ligand.<sup>33</sup> It was demonstrated that **15** is catalytically active for ammonia generation from  $\text{N}_2$  in the presence of  $\text{KC}_8$  and  $\text{HBAr}_4$  ( $\text{Ar} = 3,5-(\text{CF}_3)_2\text{C}_6\text{H}_3$ ) at low temperature. 7.0 equiv. of  $\text{NH}_3$  was obtained per Fe atom of **15**, and 44% of the added protons were delivered to  $\text{N}_2$ .<sup>34</sup> This is the first example of a molecular Fe catalyst for  $\text{NH}_3$  generation from  $\text{N}_2$ . This value was further updated to *ca.* 88 equiv. by carrying out the reaction with increased loading of the acid and the reductant under photoirradiation conditions.<sup>35</sup> Several  $\text{Fe}-\text{N}_x\text{H}_y$  complexes were isolated and structurally characterized, and their stoichiometric reactivities were also obtained.<sup>36</sup> It was confirmed that a cationic  $\text{NH}_3$ -coordinated  $\text{P}_3\text{B}$ –Fe complex **16** was formed from **15** by treatment with  $\text{HBAr}_4^{\text{F}}\cdot 2\text{Et}_2\text{O}$  and proton sponge, and **15** was regenerated by reduction of **16** with  $\text{KC}_8$  under  $\text{N}_2$  followed by further reduction with  $\text{Na}/\text{Hg}$ . It is proposed that the flexible Fe–B interaction, which varies the Fe–B distance, is important to stabilize various  $\text{Fe}-\text{N}_x\text{H}_y$  intermediates for efficient catalysis. The catalytic reactivity of the  $\text{P}_3\text{B}$ –Fe complex for hydrogenation of alkenes is also reported *via* heterolytic  $\text{H}_2$  cleavage of the Fe–B bond.<sup>37</sup>

Recently, Kameo and Bourissou reported another type of Pd–B cooperation involving anionic Pd species in a hydrodechlorination reaction of aryl chlorides.<sup>38</sup> The reaction of a Pd complex **17** having a Z-type PBP-ligand with  $\text{KH}$  and [2.2.2]-cryptand afforded an anionic Pd complex **18**, which possessed a bridging hydride ligand between Pd and B (Scheme 5). The anionic Pd complex **18** smoothly reacted with chlorobenzene to give benzene and the neutral Pd–B complex **17** whereas the



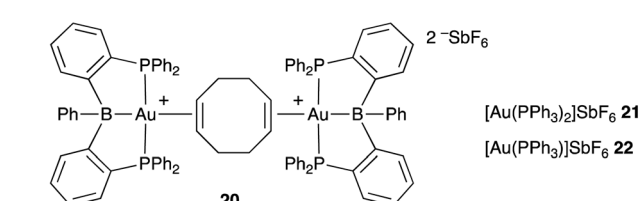
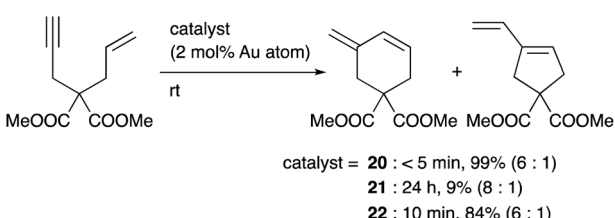
Scheme 5 Formation and reaction of the anionic PBP–Pd complex 18.



Scheme 6 Catalytic hydrodechlorination of aryl chlorides.

same oxidative addition of PhCl to **17** did not proceed at all. This was extended to a catalytic hydrodechlorination reaction of aryl chlorides with **17** or **18** using HCOOK as a reductant in the presence of [2.2.2]-cryptand (Scheme 6). Control experiments using Pd(PPh<sub>3</sub>)<sub>4</sub> with or without BPh<sub>3</sub> as an external Lewis acid resulted in low yield, suggesting a crucial cooperative effect of Pd and B on the PBP-ligand. Mechanistic studies clarified that an anionic pathway is operative; the anionic Pd<sup>0</sup> hydride complex **18** is formed first and reacts with aryl halides to give an aryl Pd<sup>II</sup> complex **19**. Intramolecular transfer of the hydride ligand from B to Pd followed by reductive elimination of a C–H bond affords the product with regeneration of the neutral Pd<sup>0</sup> complex **17**.

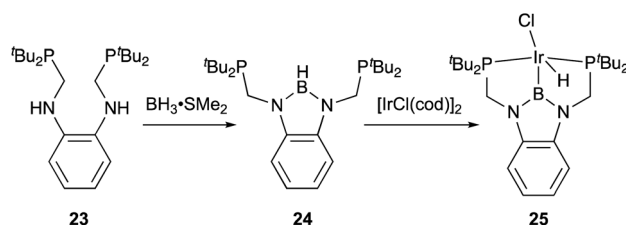
Inagaki developed a cationic Au complex **20** having a PBP-ligand, which was derived from a corresponding neutral PBP–AuCl complex originally reported by Bourissou (Scheme 7). **20** exhibited high catalytic activity for cyclization reactions of 1,*n*-enynes to give carbocycles in high yields.<sup>39</sup> The same reaction using PPh<sub>3</sub>-coordinated cationic Au complex **21** or **22** without



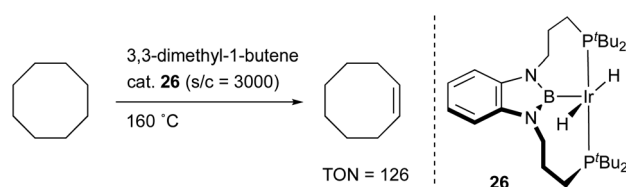
Scheme 7 Catalytic electrophilic activation of alkynes accelerated by the PBP–ligand.

the B-ligand resulted in low yields of products or required long reaction time for completion of reactions. These results clearly demonstrate a positive effect of the Z-type boron ligand in promoting the electrophilic activation of alkynes by accepting electrons from the Au center. Related electrophilic activation reactions of alkynes catalyzed by Au–B complexes were also reported.<sup>40</sup>

**3.2.2 X-type boryl ligand.** X-type boryl ligands are strong  $\sigma$ -donors and exhibit high *trans* influence.<sup>15,16</sup> These characteristics are highly promising for realizing efficient transition metal catalysis for various molecular transformations. For the synthesis of M–B complexes having an X-type boryl ligand, the tridentate PBP-ligand **12** was developed by Yamashita and Nozaki, and the synthesis and stoichiometric reactivity of its Ir complex were demonstrated.<sup>41</sup> A 1,2-bis(phosphinomethylamino)benzene derivative **23** reacted with BH<sub>3</sub> to afford bis(phosphino)-hydridoborane **24** as the PBP-ligand, which underwent oxidative addition of the B–H bond to Ir<sup>I</sup> smoothly to give the Ir–B complex **25** (Scheme 8). This method is widely applicable to the synthesis of various M–B complexes as demonstrated by the authors and other research groups later.<sup>12</sup> Yamashita reported several catalytic applications of PBP–M complexes in dehydrogenation of alkanes or dimethylamineborane, hydrosilylation of alkenes, and hydrogenation of aldehydes.<sup>42</sup> In particular, the PBP–Ir complex **26** having long-tethered P,B-linkages exhibited good catalytic activity for dehydrogenation of cyclooctane to cyclooctene (TON = 126) although the activity is lower than those with widely employed PCP–Ir complexes (Scheme 9).<sup>43</sup> López-Serrano and Rodriguez reported a hydrosilylation reaction of CO<sub>2</sub> catalyzed by a PBP–Ni complex **27** to give a bis(silyl)acetal selectively with the highest TOF (55.8 h<sup>-1</sup>) ever reported for the reaction (Fig. 4).<sup>44</sup> Zhang and Chen demonstrated the superior catalytic activity of a PBP–Pd complex **28** for a Suzuki coupling reaction to that of a corresponding PCP–Pd complex.<sup>45</sup> The strong *trans* influence and



Scheme 8 Synthesis of transition metal complexes having an X-type boryl ligand.



Scheme 9 Catalytic dehydrogenation of alkenes using the PBP–Ir complex **26**.



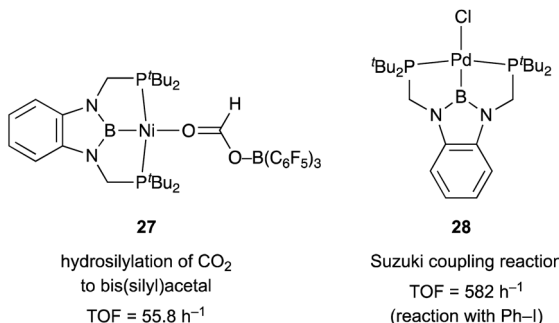
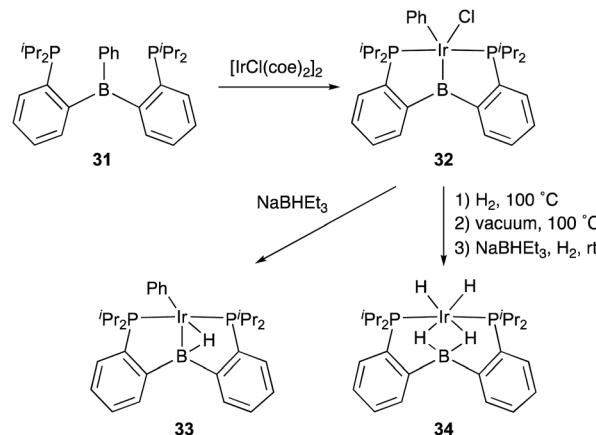


Fig. 4 Catalytic activity of PBP–Ni and PBP–Pd complexes 27 and 28.

$\sigma$ -donor ability of the boryl ligand might positively affect these reactions although the details of the reaction mechanism and the role of the boryl ligand were not clarified.

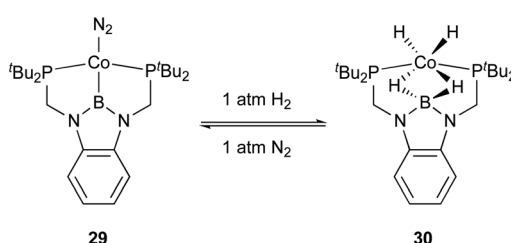
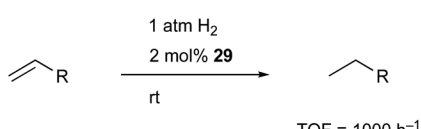
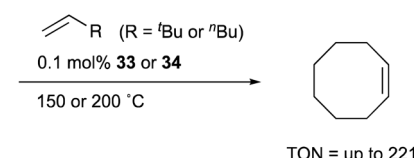
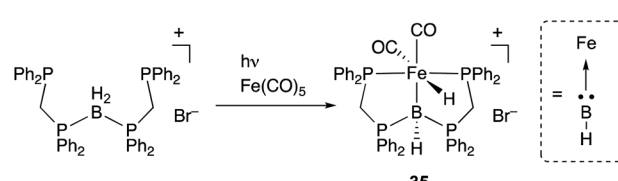
Peters utilized the PBP-ligand **24** to synthesize a PBP–Co complex **29** having an X-type boryl ligand. The Co–B complex **29** was reversibly converted to a dihydridoborate–cobalt dihydride complex **30** in the presence of 1 atm  $\text{H}_2$  (Scheme 10).<sup>46</sup> This is indicative of the cooperative activation of  $\text{H}_2$  across the Co–B bond *via* MLC. The PBP–Co complex **29** showed high catalytic activity for hydrogenation of octene and styrene, and the TOF reached 1000 per h (Scheme 11). This is a rare example of homogeneous Co-catalysis for alkene hydrogenation with high catalytic activity. The author also synthesized a bimetallic  $(\text{Co–B})_2$  complex with  $\text{PCy}_2$  side arms that exhibited better catalytic activity for hydrogenation of internal alkenes than **29**.<sup>47</sup> Synthesis and reactions of corresponding Ni–B and  $(\text{Ni–B})_2$  complexes were also demonstrated.

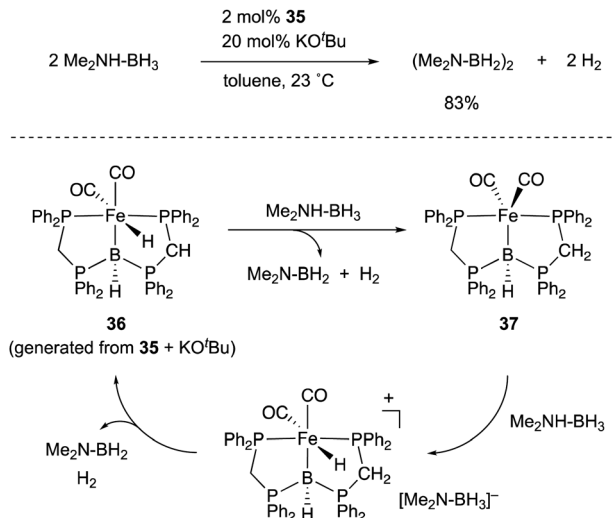
Transition metal complexes having an X-type boryl ligand stabilized by *o*-phosphinophenyl linkers have also been developed,<sup>48</sup> and their stoichiometric reactivity and catalysis were reported by Ozerov. Treatment of a PBP-ligand **31** with  $[\text{IrCl}(\text{coe})_2]_2$  afforded a PBP–Ir complex **32** *via* insertion of Ir<sup>I</sup> into a B–Ph bond (Scheme 12).<sup>49</sup> **32** was converted to Ir hydride

Scheme 12 Synthesis and reaction of the Ir–B complex **32** stabilized by *o*-phosphinophenyl linkers.

complexes **33** and **34** having bridging hydride ligands between an Ir and a B atom through reactions with  $\text{H}_2$  or  $\text{NaEt}_3\text{BH}$ . These complexes exhibited good catalytic activity for dehydrogenation of cyclooctane to cyclooctene with the maximum TON of 221, which is a better value than that for the PBP–Ir complex **26** (Scheme 13).

**3.2.3 L-type borylene ligand.** A borylene is a group 13 analogue of a carbene and coordinates to transition metals as an L-type, strong  $\sigma$ -donor ligand. There are numerous reports on the synthesis of borylene–metal complexes; however, most of them act as highly reactive borylating reagents due to the instability and high reactivity of a M–borylene moiety.<sup>18,19</sup> Therefore, suitable design of the scaffold for a M–borylene bond is necessary to stabilize and utilize a borylene as a supporting ligand in catalysis. Langer reported the synthesis of a PBP–Fe complex **35** by reaction of a boronium salt with  $\text{Fe}(\text{CO})_5$ , which proceeded *via* dissociation of CO ligands and oxidative addition of the B–H bond to Fe under photoirradiation conditions (Scheme 14).<sup>50,51</sup> Structural analysis showed that the central

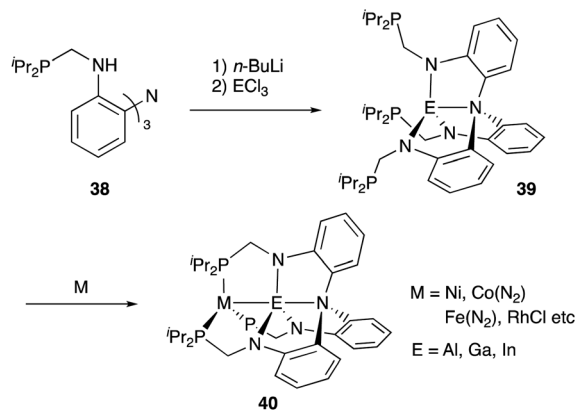
Scheme 10 Activation of  $\text{H}_2$  across the Co–B bond.Scheme 11 Hydrogenation of alkenes catalyzed by the PBP–Co complex **29**.Scheme 13 Catalytic dehydrogenation using the PBP–Ir complexes **33** and **34**.Scheme 14 Synthesis of the PBP–Fe complex **35** bearing a borylene as a supporting ligand.



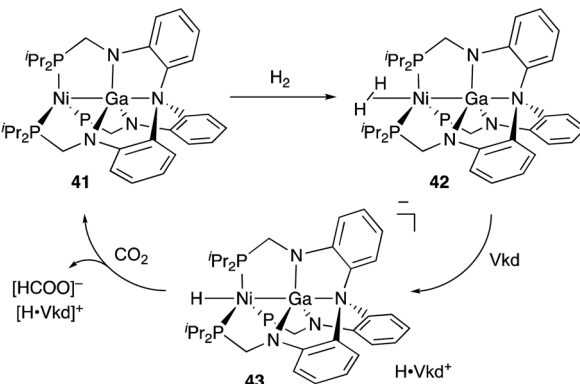
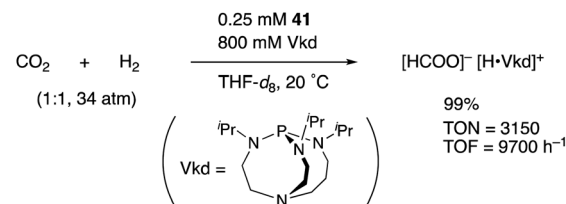
Scheme 15 Dehydrogenation of amine-borane catalyzed by the PBP-Fe complex 35.

boron atom of the Fe-B complex 35 can be best regarded as a borylene stabilized by bis(phosphino)methane linkers. The PBP-Fe complex 35 catalyzed a dehydrogenation reaction of dimethylamine-borane efficiently (Scheme 15).<sup>52</sup> Experimental and theoretical investigations indicated that the reaction mechanism involves two important steps; concerted hydrogen liberation at the anionic methine and Fe-H moieties of 36 with Me<sub>2</sub>NH-BH<sub>3</sub> to generate a neutral PBP-Fe complex 37, and protonation at the Fe center of 37 with Me<sub>2</sub>NH-BH<sub>3</sub> to regenerate 36. It is proposed that, in particular, the latter step is enhanced due to the strong electron donating ability of the borylene ligand.

**3.2.4 Al, Ga, and In as supporting ligands.** In contrast to that of M-B complexes, the catalytic application of the corresponding heavier congener M-E, where E = Al, Ga, In, and Tl, has been rather limited. This is partly due to the difficulty of incorporation and handling of highly Lewis acidic, reactive group 13 metals as supporting ligands for transition metals. In particular, the systematic synthesis of a series of M-E complexes with group 13 metals and evaluation of their catalytic reactivity have remained a formidable challenge.<sup>53</sup> Lu solved such problems by utilizing a 3-fold N,P-multidentate ligand 38 as an efficient scaffold for the M-E bond (E = Al, Ga, and In) (Scheme 16).<sup>54</sup> The successive introduction of E and M into the scaffold 38 enables facile syntheses and catalytic application of a variety of M-E complexes 40, in which the group 13 metal E acts as a  $\sigma$ -accepting Z-type ligand. They demonstrated that fine tuning of Ni for catalytic hydrogenation reactions of alkenes and carbon dioxide is possible by varying the group 13 metaloligands E, leading to development of a highly active Ni-Ga catalyst 41 for these hydrogenation reactions (Scheme 17).<sup>55,56</sup> Gallium was a better metaloligand than Al and In. In particular, a high TOF (9700 h<sup>-1</sup>) was achieved for the hydrogenation of CO<sub>2</sub> to formate under 34 atm of H<sub>2</sub>/CO<sub>2</sub> in the presence of a proazaphosphatrane base. Detailed mechanistic studies clarified that the Z-type Ga-ligand plays a crucial role in activating



Scheme 16 Efficient synthesis of M-E complexes with group 13 metaloligands 39 (E = Al, Ga, and In).

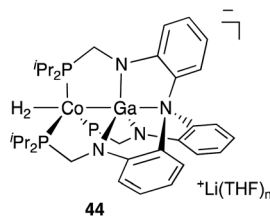


Scheme 17 Catalytic hydrogenation of CO<sub>2</sub> using the Ni-Ga complex 41.

H<sub>2</sub> electrophilically on Ni to be deprotonated by the base in an H<sub>2</sub>-coordinated Ni-Ga complex 42. The generated anionic [H-Ni-Ga]<sup>-</sup> complex 43 is a highly hydridic metal hydride species, which is efficiently stabilized through a strong Ni $\rightarrow$ Ga dative interaction. Furthermore, a related dihydrogen-coordinated anionic Ga-Co complex 44 was also synthesized and structurally characterized as another rare example of d<sup>10</sup>  $\eta^2$ -(H<sub>2</sub>)M complexes (Fig. 5).<sup>57</sup> It was demonstrated that 44 catalyzed hydrogenation of CO<sub>2</sub> efficiently *via* a Co<sup>I</sup> $\rightarrow$ Co<sup>I</sup> redox cycle, achieving a high TOF (27 000 h<sup>-1</sup>).

Recently, Lu reported catalytic hydrogenolysis of the sp<sup>2</sup>C-F bonds of aryl fluorides enabled using a Rh-In complex 45 (Scheme 18).<sup>58</sup> The reaction proceeded with a stoichiometric amount of NaO'Bu under 1 atm H<sub>2</sub> to give defluorinated arenes in good yields. Mechanistic studies supported that the Rh-In

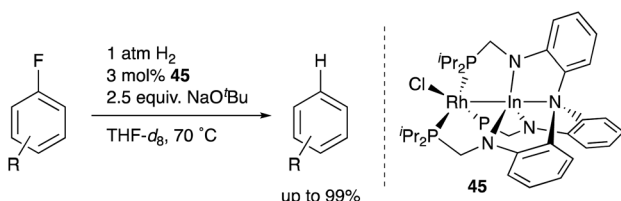




$\text{CO}_2/\text{H}_2$  (34 atm, 1:1)  
0.03 mM 42, 800 mM Vkd,  $\text{THF}-d_8$ , 293 K  
72% formate  
TOF = 27,000  $\text{h}^{-1}$

44

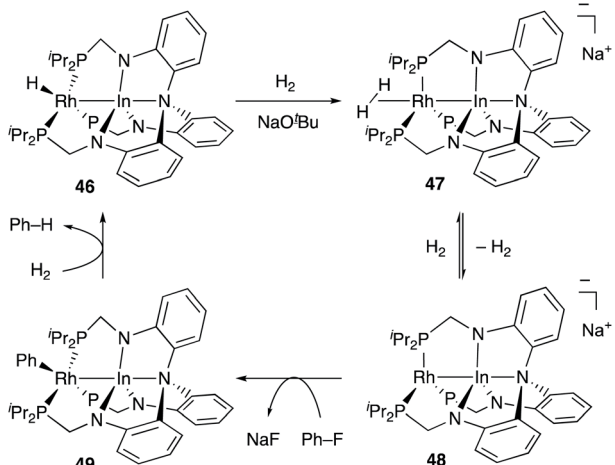
Fig. 5 Synthesis and catalytic activity of the  $\text{H}_2$ -coordinated anionic Ga-Co complex 44.



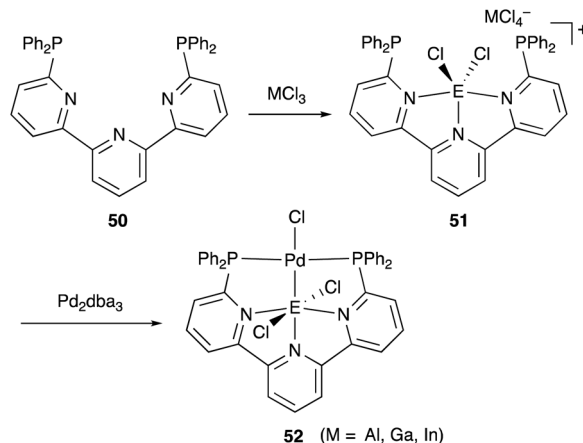
Scheme 18 Hydrogenolysis of aryl fluorides catalyzed by the Rh-In complex 45.

complex 45 is converted to a monohydride Rh-In complex 46 under the reaction conditions, which reacts with  $\text{NaOtBu}$  in the presence of  $\text{H}_2$  to generate an  $\text{H}_2$ -coordinated anionic Rh-In complex 47 (Scheme 19). The C-F bond cleavage occurs with an unsaturated rhodate complex 48 to give a phenylrhodium complex 49, and the following reaction with  $\text{H}_2$  regenerates the monohydride complex 46. These results demonstrate the high utility of the direct Rh-In interaction for the activation of strong C-F  $\sigma$ -bonds.

We have developed an efficient method for the synthesis of a variety of M-E complexes (E = Al, Ga, and In) by utilizing a 6,6''-bis(phosphino)terpyridine derivative 50 as a scaffold for the M-E bond.<sup>59</sup> The terpyridine-based rigid and planar  $\text{N}_3\text{P}_2$ -structure efficiently stabilizes the M-E bond by keeping sufficient coordination space and reactivity at the M center. The



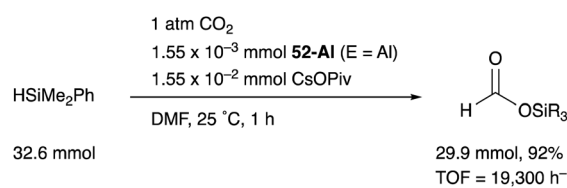
Scheme 19 Proposed reaction mechanism via the anionic Rh-In complex 48.



Scheme 20 6,6''-Bis(phosphino)terpyridine 50 as an efficient scaffold for the Pd-E bond.

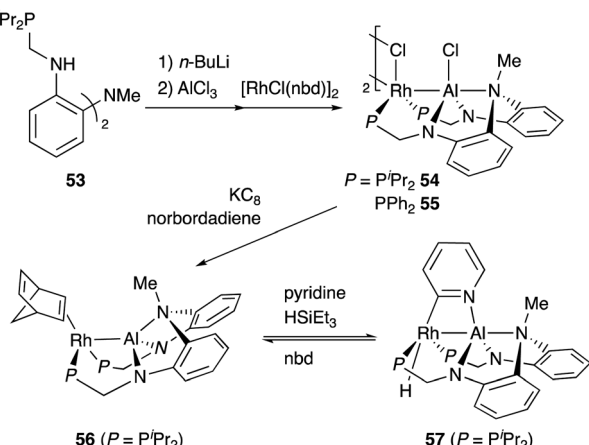
cationic [terpyridine- $\text{ECl}_2$ ]<sup>+</sup> complexes 51 act as highly electrophilic Z-type ligands, and complexation with  $\text{Pd}^0$  affords a series of Pd-E complexes 52 (Scheme 20).<sup>59a</sup> They seem to be  $\text{Pd}^{\text{II}}$  complexes having anionic Cl and PEP-pincer type ligands generated *via* redox between trivalent group 13 metals E<sup>III</sup> and  $\text{Pd}^0$ . Structural analyses showed that the Pd-Cl bond in the Pd-Al complex 52-Al is significantly elongated, suggesting the strong *trans* influence of the Al-metalloligand. The Pd-Al complex 52-Al exhibited remarkable catalytic activity for hydrosilylation of carbon dioxide to give silyl formate (Scheme 21). The reaction smoothly proceeded at room temperature under atmospheric pressure of  $\text{CO}_2$ , and the TOF reached 19 300  $\text{h}^{-1}$ , which is the highest value ever reported for this reaction. It is proposed that the *trans*-destabilizing Al-metalloligand generates highly anionic, nucleophilic Pd-H species for hydrometallation of  $\text{CO}_2$ .

Nakao developed a Rh complex 56 bearing an X-type aluminol ligand stabilized by a bis(2-(phosphinomethylamino)-phenyl)amine derivative 53.<sup>60</sup> Introduction of  $\text{AlCl}_3$  and  $\text{Rh}^{\text{I}}$  afforded a Rh complex having a Z-type Al-ligand 54, which was further reduced using  $\text{KC}_8$  in the presence of norbornadiene to give the Rh-Al complex 56 (Scheme 22).<sup>60a</sup> The C-H activation of pyridine with 56 in the presence of  $\text{HSiEt}_3$  occurred selectively at the 2-position to give a C-H cleavage product 57. This result demonstrates the sufficient Lewis acidity and high  $\sigma$ -donating ability of the Al-metalloligand for the efficient activation of a proximal C-H bond through such a Lewis acid-Lewis base interaction. According to these observations, a C2-selective

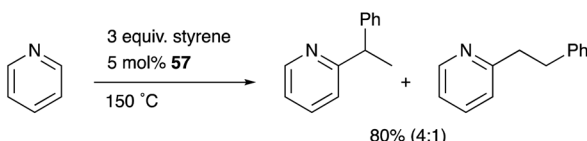


Scheme 21 Hydrosilylation of  $\text{CO}_2$  catalyzed by the Pd-Al complex 52-Al.





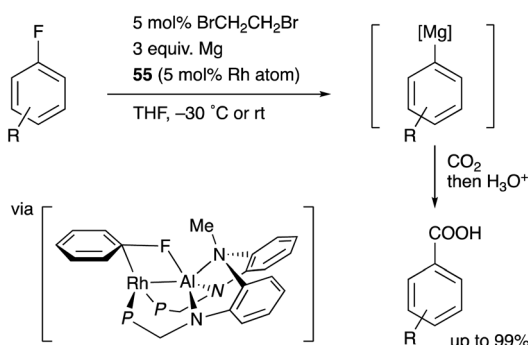
Scheme 22 Synthesis and reaction of the PAIP–Rh complex 56 having an X-type alumanyl ligand.



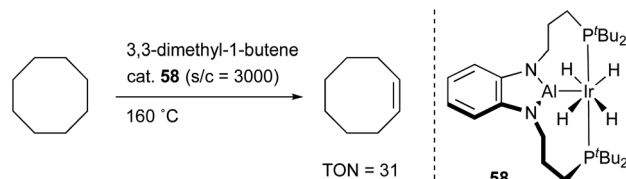
Scheme 23 57-catalyzed monoalkylation of pyridine.

mono-alkylation reaction of pyridine with alkenes catalyzed by the Rh–Al complex 57 was developed (Scheme 23).

Nakao recently reported a catalytic magnesiation reaction of aryl fluorides with Mg powder using the Rh–Al complexes 54 and 55 (Scheme 24).<sup>61</sup> The Rh–Al complex 55 having –PPh<sub>2</sub> side arms catalytically converted various aryl fluorides to arylmagnesium compounds efficiently in the presence of Mg powder and 1,2-dibromoethane, which were trapped with various electrophiles such as CO<sub>2</sub> to give carboxylic acids. This is a quite rare example of facile preparation of arylmagnesium reagents from aryl fluorides using readily available Mg powder, demonstrating the high synthetic utility of the Rh–Al catalyst. The catalyst 54 was confirmed to be reduced with Mg to generate the low-valent Rh–Al complex 56 in the presence of norbornene. Based on these experimental studies and theoretical



Scheme 24 PAIP–Rh complex-catalyzed magnesiation of aryl fluorides.

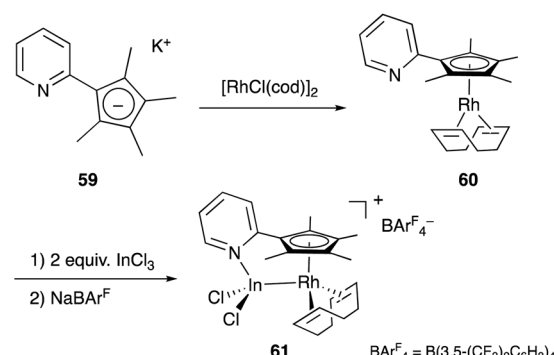


Scheme 25 PAIP–Ir 58-catalyzed dehydrogenation of alkanes.

calculations, it was proposed that the oxidative addition of the inert sp<sup>2</sup>C–F bond occurred across the Rh–Al bond of a low valent Rh–Al complex.

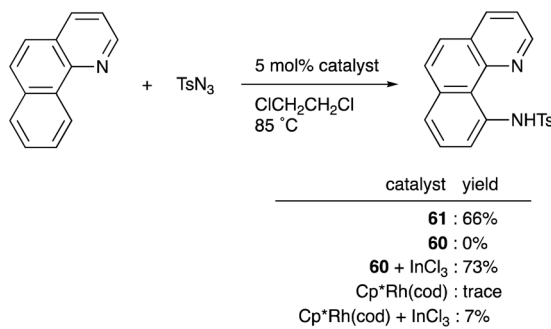
Yamashita reported the synthesis and catalytic activity of an Ir complex 58 with an X-type PAIP-ligand using the same scaffold employed for the PBP–Ir complexes 26 (Scheme 25).<sup>62</sup> The tricoordinate Al-ligand is demonstrated to act as a Lewis acid to capture a Lewis base such as DMAP. Catalytic application of the Ir–Al complex 58 to a dehydrogenation reaction of cyclooctane to cyclooctene was investigated although the activity was not satisfactory.

Recently, a different approach to M–E complexes with heavier group 13 elements has been established by our group. A Cp–rhodium complex 61 having a cationic InCl<sub>3</sub><sup>+</sup> metalloligand was synthesized through the reaction of 2 equivalents of InCl<sub>3</sub> and a Rh<sup>I</sup> complex 60, which was prepared from a pyridine-tethered Cp derivative 59 (Scheme 26).<sup>63</sup> This method enables post-introduction of a group 13 metalloligand to a Cp–metal complex to form an M–E bond, which is distinct from the pre-introduction approaches described before. Therefore, screening of metalloligands becomes possible for the development of catalytic reactions. The cationic In–metalloligand acts as a strong σ-acceptor for Rh, and theoretical calculations and CV measurements revealed that the electronic and redox properties of the Rh in 61 become similar to those of trivalent Cp\*Rh<sup>III</sup> rather than those of the original monovalent Rh<sup>I</sup> complex 60 through the formation of the Rh–In bond. This was also demonstrated in catalysis. The Rh–In complex 61 catalyzed sp<sup>2</sup>C–H amidation of benzo[*h*]quinoline with TsN<sub>3</sub> to afford an *N*-aryltosylamide derivative in good yield (Scheme 27). Control experiments employing Cp\*Rh(cod) or 60 with or without InCl<sub>3</sub>



Scheme 26 Synthesis of the Rh–In complex 61 via post-introduction of a group 13 metalloligand.



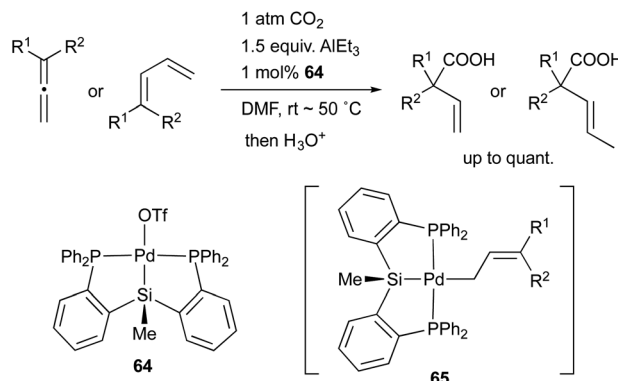
Scheme 27  $sp^2$ C–H activation enabled using the In-metalloligand.

as catalysts supported the unique reactivity of the Rh–In bond to turn on the C–H activation catalysis. The reaction was also applicable to various arenes having pyridine or pyrimidine as a directing group. These results demonstrate the promising utility of this approach in exploring new transition metal catalysis with M–E bonds in synthetic chemistry.

### 3.3 Group 14 (E = Si and Ge)

Transition metal complexes having a silyl ligand as an anionic X-type ligand have been extensively studied since they are important intermediates in various catalytic silylation reactions such as hydrosilylation and C–H silylation.<sup>64</sup> The silyl ligand is expected to act as a strong  $\sigma$ -donor and a *trans* influencing ligand.<sup>15,16</sup> MLC on the M–Si bond can also be considered.<sup>24</sup>

Various Si-containing multidentate ligands and their transition metal complexes have been developed including tri- and tetradeятate phosphinosilyl ligands tethered using alkyl or o-phenylene linkers, an NSiN-type bis(8-quinolyl)silyl ligand, polyisilyl ligands and so on.<sup>14</sup> Although catalytic applications were demonstrated in hydroformylation, hydrogenation, hydrosilylation, hydroboration, C–H silylation reactions *etc.*, the

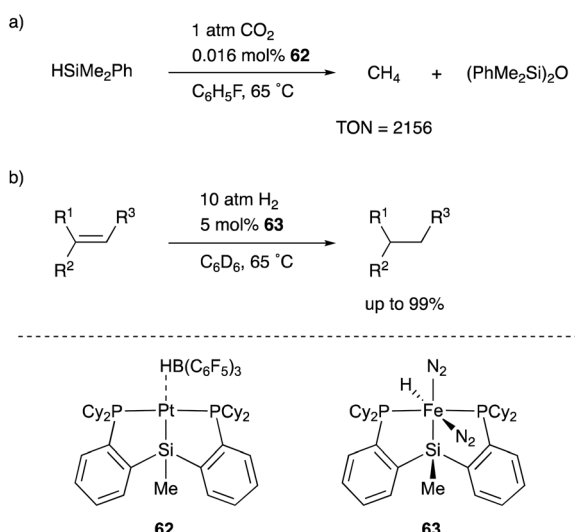


Scheme 29 Hydrocarboxylation of simple unsaturated hydrocarbons catalyzed by the PSiP–Pd complex 64.

efficiency and selectivity of the catalysis were not necessarily advantageous compared with those of standard transition metal catalysts without silyl ligands.<sup>65</sup> Selected examples of unusual molecular transformations and catalytic activity enabled using silyl ligands are described.

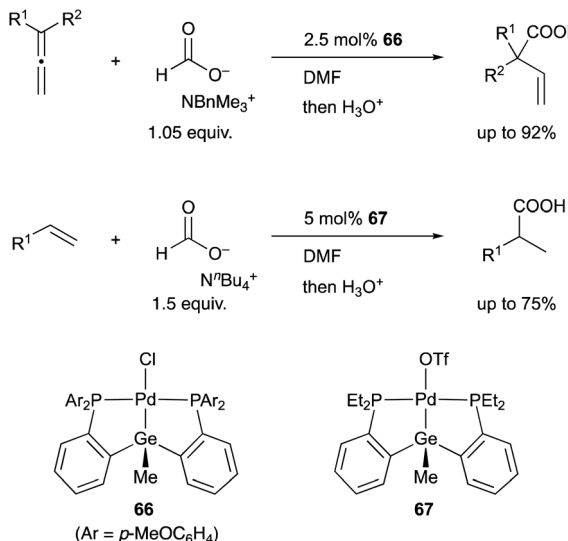
One of the most versatile multidentate Si-ligands used for transition metal catalysts is a bis(phosphinophenyl)silyl derivative (phenylene-bridged PSiP-ligand). Turculet reported the synthesis of various transition metal complexes having a PSiP-ligand in 2007 for the first time. Several catalytic applications were also examined by Turculet and other research groups, and high catalytic activity and unusual molecular transformations taking advantage of the silyl ligand are achieved in some cases. For example, a PSiP–Pt complex 62 catalyzed the reduction of CO<sub>2</sub> to methane with HSiMe<sub>2</sub>Ph under mild reaction conditions (1 atm, 65 °C), and the TON reached 2156 (Scheme 28).<sup>66</sup> The pincer-type PSiP-ligand was also applicable to first row transition metals such as Fe, and the catalytic activity of a PSiP–Fe hydride complex 63 for hydrogenation of alkenes with H<sub>2</sub> (10 atm) was demonstrated as a relatively rare example of Fe-catalysts for the reaction.<sup>67</sup>

In 2008, we developed a PSiP–Pd complex 64-catalyzed hydrocarboxylation reaction of alkenes and 1,3-dienes under atmospheric pressure of CO<sub>2</sub> using AlEt<sub>3</sub> as a stoichiometric reductant (Scheme 29).<sup>68</sup> This is a new CO<sub>2</sub>-fixation reaction using simple unsaturated hydrocarbons as substrates to give synthetically useful  $\beta,\gamma$ -unsaturated carboxylic acids selectively in high yields. Hydrometallation of a C–C double bond generates a highly nucleophilic  $\sigma$ -allylpalladium complex 65, which smoothly reacts with a less reactive molecule, CO<sub>2</sub>, even at room temperature because of the strong  $\sigma$ -donating ability and *trans* influence of the silyl ligand.<sup>69</sup> Furthermore, we also realized atom-economical hydrocarboxylation reactions of alkenes and alkynes employing a formate salt as a reductant as well as a CO<sub>2</sub> source enabled using newly developed Pd complexes 66 and 67 bearing a PGeP-pincer type ligand (Scheme 30).<sup>70</sup> This reaction proceeds under mild conditions and provides an alternative strategy for utilizing formate salts as a C1 source. These reactions did not proceed with standard Pd complexes and PCP- and PNP–Pd complexes, thus clearly demonstrating the privileged reactivity of the Pd–Si and Pd–Ge bonds in catalysis.



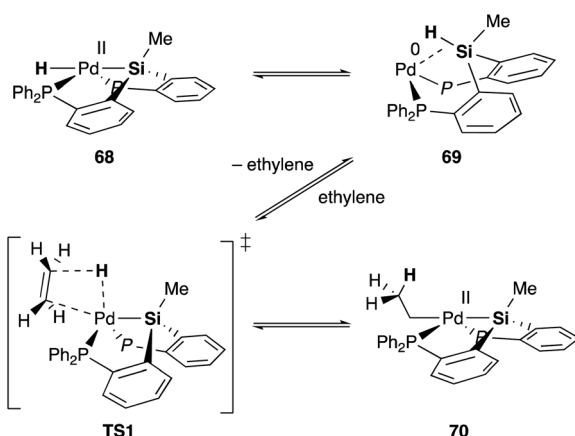
Scheme 28 Hydrosilylation and hydrogenation reactions catalyzed by PSiP–M complexes.



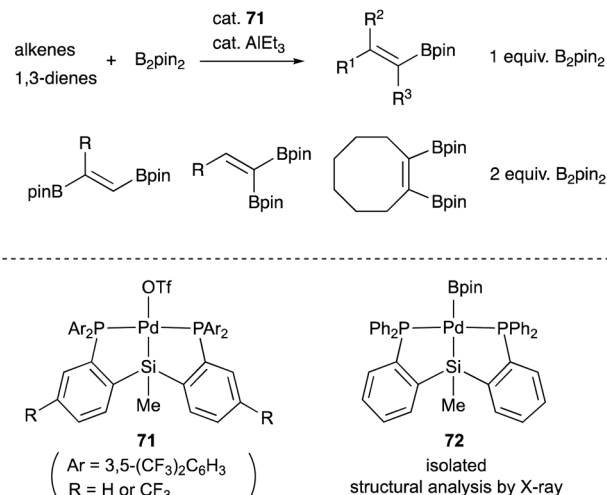


Scheme 30 PGeP–Pd complex **66** or **67**-catalyzed hydrocarboxylation using a formate salt as both a reductant and  $\text{CO}_2$  source.

Silyl and germyl ligands play important roles not only in promoting the nucleophilic addition step, but also in enabling a new hydrometallation mechanism *via* MLC. Mechanistic studies using ethylene as a model substrate clarified that an  $\eta^2$ -(E–H)Pd<sup>0</sup> complex **69**, which is reversibly generated *via* reductive elimination of an E–H bond from a Pd<sup>II</sup> hydride complex **68**, undergoes associative hydrometallation *via* a 5-coordinated TS1 to afford an ethyl-Pd<sup>II</sup> complex **70** directly without dissociation of one of the –PR<sub>2</sub> side arms (Scheme 31).<sup>71</sup> During the reaction, the PEP-pincer ligand acts as an efficient scaffold for delivering the hydrogen atom as a hydride ligand between E and Pd accompanied by the formation and cleavage of the Pd–E bond. This is an unusual mechanism for hydrometallation and  $\beta$ -hydrogen elimination *via* MLC of the Pd–Si bond, demonstrating the promising utility of the Si-ligand in transition metal catalysis. It is also clarified that the germyl ligand stabilizes the ethyl-Pd<sup>II</sup> state more efficiently than the silyl ligand



Scheme 31 Associative hydrometallation/β-hydrogen elimination *via* MLC of the Pd–Si bond.

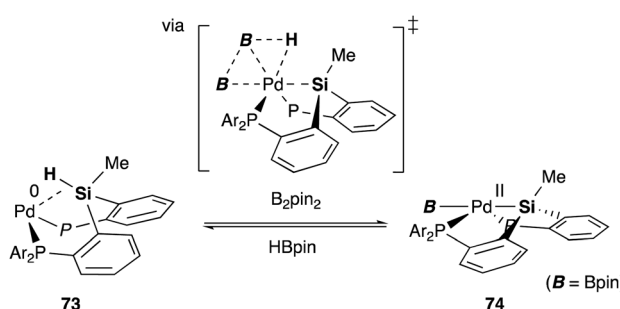


Scheme 32 Selective single or double dehydrogenative borylation of alkenes catalyzed by the PSiP–Pd complex **71**.

and is suitable for reactions with formate salts under heating conditions.<sup>72</sup>

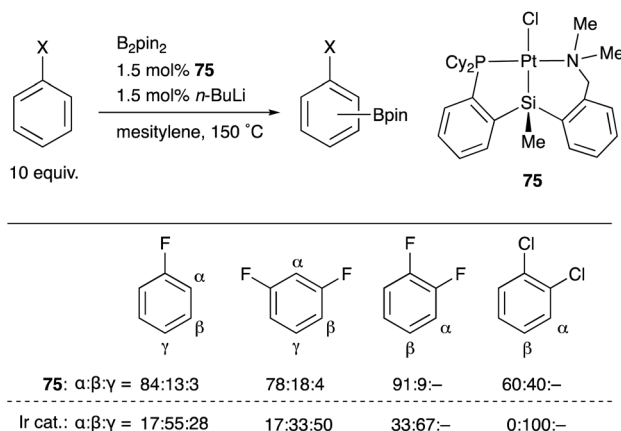
We have also developed a selective dehydrogenative borylation reaction of alkenes with B<sub>2</sub>pin<sub>2</sub> catalyzed by PSiP–Pd complex **71** having electron deficient Ar substituents on phosphorus side arms (Scheme 32). The reaction with 2 equivalents of B<sub>2</sub>pin<sub>2</sub> enables an efficient synthesis of a variety of double borylation products involving 1,1-, *trans*-1,2-, and cyclic-1,2-diborylalkenes starting from alkenes and B<sub>2</sub>pin<sub>2</sub>, which are synthetically highly useful but not accessible with standard transition metal-catalyzed borylation reactions.<sup>73</sup> It is clarified that the reaction proceeds *via* a borylpalladium complex **72** having a PSiP-pincer type ligand, which possesses an elongated and highly reactive Pd–B bond due to the strong *trans* influence of the silyl ligand as evidenced by X-ray analysis and stoichiometric reactivity studies. Detailed mechanistic studies revealed that a reversible  $\sigma$ -bond metathesis reaction is operative between an  $\eta^2$ -(Si–H)Pd<sup>0</sup> complex **73** and B<sub>2</sub>pin<sub>2</sub> to form a borylpalladium complex **74** through MLC similar to the case of the hydrocarboxylation reaction (Scheme 33).<sup>74</sup>

We have designed and synthesized a platinum complex **75** having a PSiN-pincer type ligand, in which one of the *o*-



Scheme 33 Reversible  $\sigma$ -bond metathesis of the  $\eta^2$ -(Si–H)Pd<sup>0</sup> complex **73** with B<sub>2</sub>pin<sub>2</sub>.





Scheme 34 Regioselective C–H borylation of fluoro- and chloroarenes catalyzed by the PSiN–Pt complex 75.

phosphinophenyl linkages is replaced by an *o*-(aminomethyl)phenyl group expecting the lability of the Pt–N bond to generate a coordinatively unsaturated 14e Pt center (Scheme 34).<sup>75</sup> The PSiN–Pt complex catalyzed  $sp^2$ C–H borylation of various electron deficient arenes such as fluoro- or chloroarenes efficiently, affording halogenated arylboronic esters in good yields. This is a quite rare example of Pt-catalyzed  $sp^2$ C–H borylation.<sup>76</sup> Interestingly, the borylation occurs at a C–H bond adjacent to the halogen substituent preferentially. This regioselectivity is in sharp contrast to that of Ir-catalyzed borylation, in which borylation tends to occur at less sterically hindered C–H bonds as shown in the table. Although the reaction mechanism and the origin of the regioselectivity are not clear yet, these results demonstrate the unique catalytic activity of Pt–Si complexes in synthetic chemistry.

Tobita developed a bis(silyl)-chelate ligand, xantsil 76, based on a xanthene backbone, which possesses a wide bite-angle and exhibits strong  $\sigma$ -donation ability and *trans* influence. The xantsil–Ru complex 77 catalyzed an unusual hydrosilylation reaction of arylacetylenes with silane, in which *ortho*-C–H silylation of the aryl moiety occurs accompanied by *trans*-hydrogenation of the C–C triple bond to give *trans*-(*o*-silylaryl)alkenes

(Scheme 35).<sup>77</sup> It is proposed that one of the silyl ligands fluxionally dissociates from Ru after oxidative addition of a C–H bond and reforms after the formation of the product during the reaction. Slight modification of the substituents on the phosphorus ligand switched the reaction pathway to tandem hydrosilylation/C–H silylation of alkynes to give bis(silylated) stilbene derivatives.<sup>78</sup>

A silylene and a germylene, which are heavier analogues of a carbene, have also been utilized as a supporting ligand for transition metal catalysts. Driess and Hartwig developed ECE-type multidentate ligands possessing two base-stabilized silylene or germylene moieties as side arms (E = Si or Ge), and catalytic application of their Ir and Ni complexes was reported (Fig. 6).<sup>79</sup> The SiCSi–Ir complex 78–Si exhibited higher efficiency for a catalytic C–H borylation reaction of benzene than the corresponding Ir complex having a PCP-pincer type ligand possibly due to the stronger  $\sigma$ -donating ability of the Si<sup>II</sup> ligand than the P<sup>III</sup> ligand (Scheme 36).<sup>79a</sup> Moreover, the SiCSi–Ni

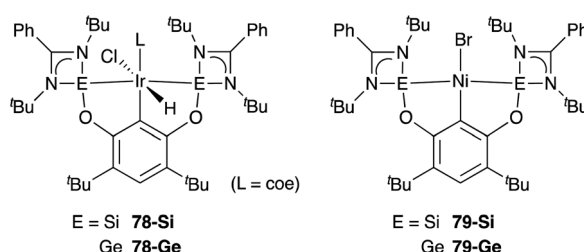
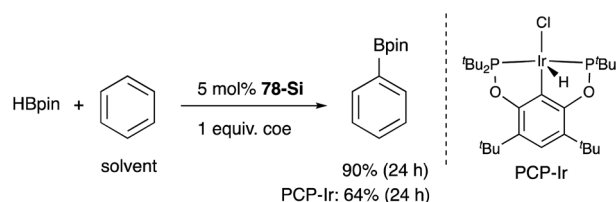
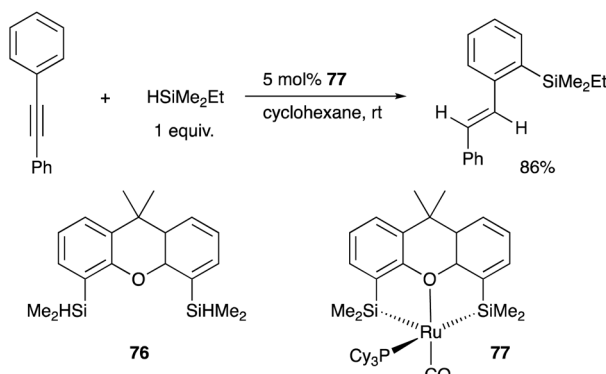


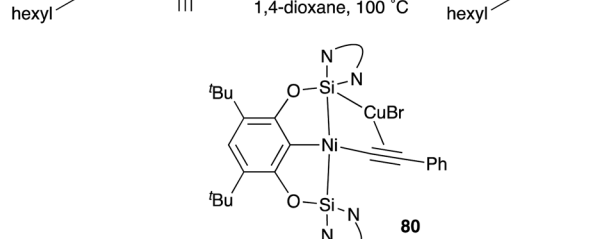
Fig. 6 Silylenes and germylenes as supporting ligands for transition metal catalysts.



Scheme 36  $sp^2$ C–H borylation catalyzed by the bis(silylene)–Ir complex 78–Si.



Scheme 35 Tandem hydrogenation/C–H silylation catalyzed by the xantsil–Ru complex 77.



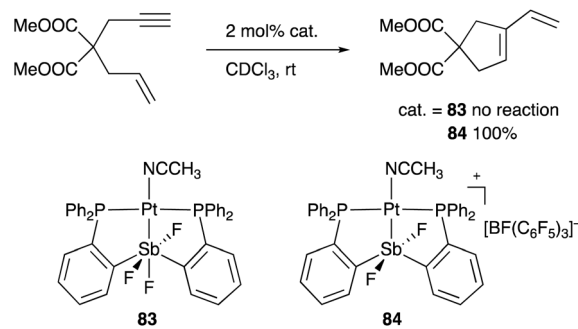
Scheme 37 The SiCSi–Ni complex 79–Si-catalyzed Sonogashira coupling reaction.

complex **79-Si** catalyzed the Sonogashira coupling reaction of an alkenyl iodide and an alkyne (Scheme 37).<sup>79b</sup> Mechanistic studies clarified that the reaction proceeded through the sequence of transmetalation, oxidative addition, and reductive elimination. As an important intermediate, an alkynylnickel complex **80** was isolated and structurally characterized, in which CuBr coordinates to one of the silylene ligands and an alkyne moiety. Although the catalysis in these reactions is not tremendous yet, these results demonstrate the promising utility of group 14 metallylenes as a unique donor ligand in transition metal catalysis.

### 3.4 Group 15 (E = Sb and Bi)

Heavier group 15 elements such as Sb and Bi possess distinct electronic characteristics and reactivities from those of lighter pnictogens such N and P. The  $\sigma$ -donating ability of trivalent Sb and Bi compounds  $ER_3$  (E = Sb and Bi) is weak due to the stabilized 5s and 6s electrons by the relativistic contraction. Scrambling and transfer of the substituent R on E are often observed due to the relatively weak and reactive E–C bond. Therefore, the number of transition metal complexes having L-type, trivalent Sb- and Bi-ligands and their catalytic applications have been rather limited compared with those of phosphine ligands.<sup>80</sup> On the other hand, trivalent Sb and Bi compounds often behave as Lewis acids, enabling Z-type coordination to Lewis basic transition metals.<sup>81</sup> Moreover, redox between  $E^{III}$  and  $E^V$  and coordination/dissociation of ligands on E enable modular tuning of electronic and steric properties of these compounds. These characteristics are highly promising for developing multi-functional transition metal catalysts, where the reactivity of the transition metal is tunable with chemical stimuli on E.

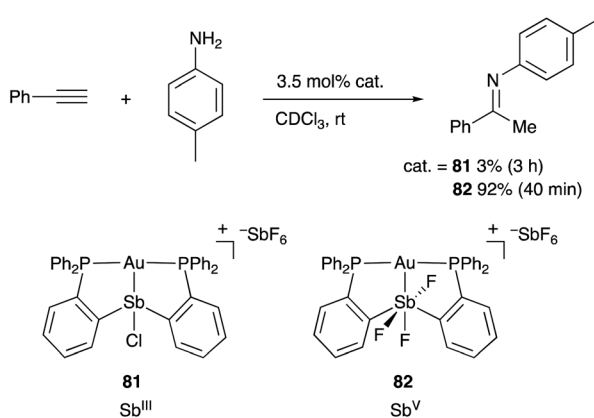
Gabbaï reported the synthesis and catalytic application of various Au and Pt complexes having an Sb-ligand.<sup>8,9,82</sup> The o-phosphinophenyl linkage is often utilized as a support for the M–Sb bond. The Sb atom acts as a non-innocent Z-type ligand, where its  $\sigma$ -accepting ability is tunable by changing the oxidation state and substituents on Sb for various electrophilic activation reactions of C–C triple bonds. For example, the cationic



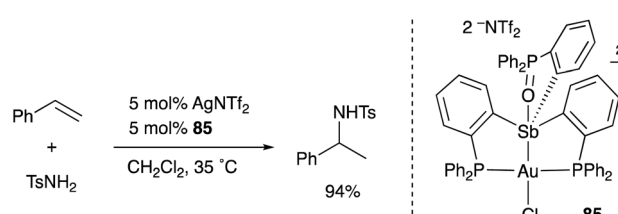
Scheme 39 The PSbP–Pt complex **84** activated by abstraction of a fluoride ligand on Sb.

PSbP–Au complex **81** having a trivalent Sb<sup>III</sup>-ligand scarcely catalyzed hydroamination of alkynes to give an imine product in very low yield (Scheme 38).<sup>83</sup> On the other hand, the catalytic activity dramatically increased by oxidizing the Sb<sup>III</sup>-ligand to a pentavalent Sb<sup>V</sup>-ligand in **82**, giving the product in 92% yield within 40 min. It is conceivable that the electronically positive, pentavalent Sb<sup>V</sup>-ligand makes the Au atom more electrophilic than the trivalent Sb<sup>III</sup>-ligand to promote the electrophilic activation of alkynes efficiently.

A neutral PSbP–Pt complex **83** bearing a pentavalent Sb<sup>V</sup>-ligand was activated electrophilically by abstracting one of the fluorine ligands on Sb<sup>V</sup> (Scheme 39).<sup>84</sup> The activated form, a cationic PSbP–Pt complex **84**, efficiently catalyzed an electrophilic cyclization reaction of 1,6-enynes to form carbocycles in good yields. The cationic Sb moiety serves as a strong  $\alpha$ -acceptor, increasing the  $\pi$ - acidity of the Pt complex for efficient electrophilic activation of alkynes. Similar reactivity control on Sb was also demonstrated in the case of a PSbP–Au complex **85**. Introduction of a phosphine oxide side arm on Sb enables the generation of a dicationic Sb<sup>V</sup>-ligand, which makes the Au atom highly electrophilic. The dicationic PSbP–Au complex **85** catalyzed hydroamination and polymerization of styrene derivatives efficiently (Scheme 40).<sup>85</sup> Furthermore, self-activation of the catalytic activity of a PSbP–Pt complex **86** for electrophilic activation reactions was also reported (Scheme 41).<sup>86</sup> It is proposed that abstraction of a chloride ligand on Pt using the electrophilic Sb-ligand generates a cationic PSbP–Pt complex **87** as a reactive intermediate, which was supported by isolation and structural analysis of a related dicationic PSbP–Pt complex with L = CyCN. These examples showed that efficient control of transition metal catalysis is possible by utilizing characteristic

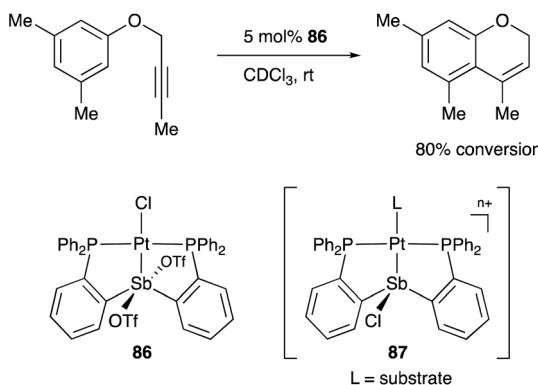


Scheme 38 Electrophilic activation of alkynes catalyzed by the Au–Sb complex **82** having the redox non-innocent PSbP-ligand.



Scheme 40 Catalytic electrophilic activation of alkenes enabled using the dicationic Sb-ligand in the PSbP–Au complex **85**.



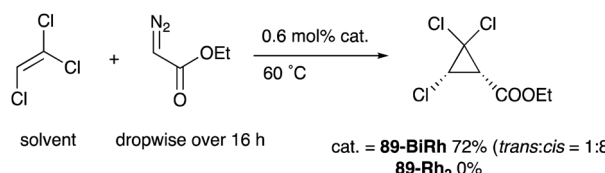
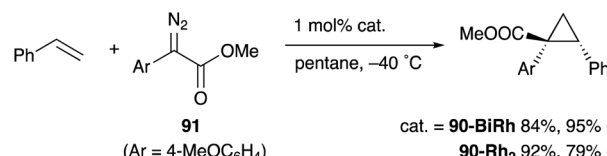


Scheme 41 Self-activation of Pt-catalysis with the Sb-ligand.

Lewis acidity and redox and coordination behaviors of the Sb ligand, demonstrating the practical utility of the non-innocent Sb-ligand in synthetic chemistry.

Regarding Bi-containing multidentate ligands, a related analogue, bis(*o*-phosphinophenyl)chlorobismuth(III), has been developed, and synthesis and structural analysis of Au, Pt, Pd, Cu, and Ag complexes having the PBiP-ligand were reported by Gabbaï and Limberg.<sup>87,88</sup> It was revealed that the central Bi<sup>III</sup> atom acts as a  $\sigma$ -acceptor for Au, Pt, and Pd rather than as a  $\sigma$ -donor while the Bi $\rightarrow$ M interaction is dominant for Cu and Ag. Limberg also developed another Bi-containing multidentate ligand based on xanthene.<sup>89</sup> However, the catalytic reactivity of these complexes for synthetic reactions has not been investigated.

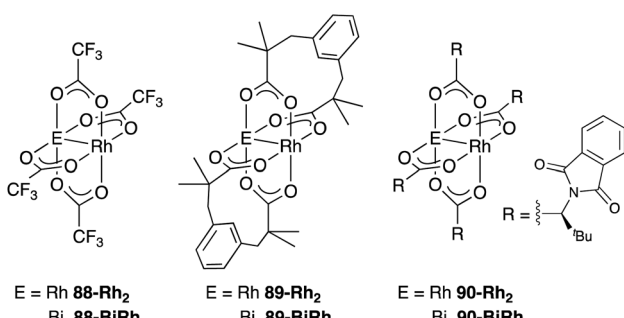
As a related example of M-Bi complexes, heterobimetallic paddlewheel Bi-Rh carboxylate complexes BiRh(X)<sub>4</sub> have been developed by Dikarev,<sup>90</sup> where one of the 4d Rh atoms of the well-known paddlewheel Rh<sub>2</sub>(X)<sub>4</sub> complex was replaced by a 6p Bi (Fig. 7). The parent Rh<sub>2</sub>(X)<sub>4</sub> complexes are widely utilized as efficient catalysts for carbene transfer reactions of diazo compounds. The catalytic activity of the BiRh(X)<sub>4</sub> complexes has been evaluated in the carbene transfer reactions to elucidate the effect of the Bi-ligand on the reactivity. Davies reported the catalytic activity of various paddlewheel Bi-Rh complexes in cyclopropanation and C-H activation reactions and commented that decomposition of a diazo compound became slower with the Bi-Rh complex **88-BiRh** than **88-Rh<sub>2</sub>**.<sup>91</sup> Recently, Fürstner

Scheme 42 Cyclopropanation of electron deficient alkenes catalyzed by the Bi-Rh complex **89-BiRh**.Scheme 43 The Bi-Rh complex **90-BiRh**-catalyzed asymmetric cyclopropanation of styrenes.

developed a Bi-Rh complex **89-BiRh** and realized catalytic cyclopropanation of highly electron-deficient polychlorinated alkenes such as trichloroethylene, which were not employable substrates in the previously reported Rh<sub>2</sub>-catalyzed reactions (Scheme 42).<sup>92</sup> Experimental analyses and theoretical calculations on the structure and electronic properties of the Bi-Rh bimetallic complexes showed that the carbene moiety becomes electrophilic because back donation of electrons from Rh to the carbene is reduced in the Bi-Rh complex. Furthermore, the chiral version of the Bi-Rh complex **90-BiRh** having a *tert*-leucine derivative as bridging carboxylate ligands was also developed and applied to an asymmetric cyclopropanation reaction of styrenes (Scheme 43).<sup>93</sup> The Bi-Rh complex **90-BiRh** achieved better enantioselectivity in the reactions of a diazo compound **91** than that with a standard Rh<sub>2</sub> catalyst **90-Rh<sub>2</sub>** due to the more confined, effective chiral space produced by the Bi-Rh core.

#### 4. Conclusions and perspectives

Recent progress on catalytic application of transition metal complexes having an M-E bond (E = main group metal or metalloid element) is summarized. Several important scaffolds for M-E bonds have been established to enable efficient synthesis of a variety of M-E complexes and their utilization as catalysts in synthetic reactions. Main group metal and metalloid supporting ligands E furnish unusual electronic and steric environments and molecular functions to the transition metals, in particular through Z-type ligation and MLC of the M-E bonds, which are not easily available with standard organic supporting ligands such as phosphines and amines. These characteristics lead to remarkable catalytic activity and product selectivity in some cases. The reactivity control with the chemical stimuli on E-ligands is also intriguing to develop a multi-functional transition metal catalyst that changes its reactivity depending on the environment. This progress demonstrates the importance and synthetic utility of main group metal and



Scheme 7 Paddlewheel Bi-Rh complexes.



metalloid supporting ligands in organometallic and synthetic chemistry.

Besides the examples described in this article, there are numerous reports on the synthesis and stoichiometric reactivity of M–E complexes, which are potentially applicable to catalytic reactions. Investigation on the catalytic activity of other M–E complexes including group 16 elements or other heavier elements as E-ligands is also of great interest. An important future challenge is to realize new and synthetically valuable molecular transformations, which are not easily achieved with the standard transition metal catalysts, exploiting the characteristic reactivity of M–E complexes from the viewpoint of synthetic chemistry. In particular, strategic utilization of MLC for activation of unreactive chemical bonds and molecules based on the rational design of the ligand structure will be important. Further exploration will ensure successful utilization of M–E complexes as a new class of transition metal catalysts.

## Conflicts of interest

There are no conflicts to declare.

## Acknowledgements

The author thanks JSPS KAKENHI grant numbers 17H03019, 20H02732, 18H04646, 20H04806, and JST, PRESTO grant number JY290145, Japan for financial support.

## Notes and references

- 1 M. Stradiotto, *Ligand Design in Metal Chemistry: Reactivity and Catalysis*, Wiley, 2016.
- 2 (a) A. J. Arduengo, R. L. Harlow and M. Kline, *J. Am. Chem. Soc.*, 1991, **113**, 361–363; (b) W. A. Herrmann and C. Köcher, *Angew. Chem., Int. Ed.*, 1997, **36**, 2162–2187; (c) F. E. Hahn and M. C. Jahnke, *Angew. Chem., Int. Ed.*, 2008, **47**, 3122–3172; (d) S. P. Nolan, *N-Heterocyclic Carbenes*, Wiley, 2014.
- 3 G. Bouhadir and D. Bourissou, *Chem. Soc. Rev.*, 2015, **45**, 1065–1079.
- 4 G. Parkin, *Organometallics*, 2006, **25**, 4744–4747.
- 5 A. Amgoune and D. Bourissou, *Chem. Commun.*, 2011, **47**, 859–871.
- 6 H. Kameo and H. Nakazawa, *Chem.-Asian J.*, 2013, **8**, 1720–1734.
- 7 H. Kameo and H. Nakazawa, *Chem. Rec.*, 2017, **17**, 268–286.
- 8 S. J. Jones and F. P. Gabbaï, *Acc. Chem. Res.*, 2016, **49**, 857–867.
- 9 D. You and F. P. Gabbaï, *Trends Chem.*, 2019, **1**, 485–496.
- 10 S. Aldridge and D. L. Coombs, *Coord. Chem. Rev.*, 2004, **248**, 535–559.
- 11 H. Braunschweig, R. D. Dewhurst and A. Schneider, *Chem. Rev.*, 2010, **110**, 3924–3957.
- 12 M. Yamashita, *Bull. Chem. Soc. Jpn.*, 2016, **89**, 269–281.
- 13 M. S. Balakrishna, P. Chandrasekaran and P. P. George, *Coord. Chem. Rev.*, 2003, **241**, 87–117.
- 14 M. Simon and F. Breher, *Dalton Trans.*, 2017, **46**, 7976–7997.
- 15 T. G. Appleton, H. C. Clark and L. E. Manzer, *Coord. Chem. Rev.*, 1973, **10**, 335–422.
- 16 J. Zhu, Z. Lin and T. B. Marder, *Inorg. Chem.*, 2005, **44**, 9384–9390.
- 17 M. Asay, C. Jones and M. Driess, *Chem. Rev.*, 2011, **111**, 354–396.
- 18 H. Braunschweig, R. D. Dewhurst and V. H. Gessner, *Chem. Soc. Rev.*, 2013, **42**, 3197–3208.
- 19 H. Braunschweig and R. Shang, *Inorg. Chem.*, 2015, **54**, 3099–3106.
- 20 J. T. Goettel and H. Braunschweig, *Coord. Chem. Rev.*, 2019, **380**, 184–200.
- 21 P. W. Roesky, *Dalton Trans.*, 2009, 1887–1893.
- 22 D. Vidovic and S. Aldridge, *Chem. Sci.*, 2011, **2**, 601–608.
- 23 J. R. Khusnutdinova and D. Milstein, *Angew. Chem., Int. Ed.*, 2015, **54**, 12236–12273.
- 24 R. N. Perutz and S. Sabo-Etienne, *Angew. Chem., Int. Ed.*, 2007, **46**, 2578–2592.
- 25 For selected examples, see; (a) M. Bennett, M. Contel, D. C. R. Hockless and L. L. Welling, *Chem. Commun.*, 1998, 2401–2402; (b) A. C. Kuate, R. A. Lalancette, T. Bannenberg and F. Jäkle, *Angew. Chem., Int. Ed.*, 2018, **57**, 6552–6557 and references cited therein.
- 26 P. Steinhoff, M. Paul, J. P. Schroers and M. E. Tauchert, *Dalton Trans.*, 2018, **48**, 1017–1022.
- 27 (a) N. Tsoureas, G. R. Owen, A. Hamilton and A. G. Orpen, *Dalton Trans.*, 2008, 6039–6044; (b) N. Tsoureas, Y.-Y. Kuo, M. F. Haddow and G. R. Owen, *Chem. Commun.*, 2010, **47**, 484–486; (c) M. E. El-Zaria, H. Arii and H. Nakamura, *Inorg. Chem.*, 2011, **50**, 4149–4161; (d) H. Kameo and H. Nakazawa, *Organometallics*, 2012, **31**, 7476–7484; (e) T. Schindler, M. Lux, M. Peters, L. T. Scharf, H. Osseili, L. Maron and M. E. Tauchert, *Organometallics*, 2015, **34**, 1978–1984.
- 28 (a) S. Bontemps, G. Bouhadir, K. Miqueu and D. Bourissou, *J. Am. Chem. Soc.*, 2006, **128**, 12056–12057; (b) S. Bontemps, H. Gornitzka, G. Bouhadir, K. Miqueu and D. Bourissou, *Angew. Chem., Int. Ed.*, 2006, **45**, 1611–1614; (c) S. Bontemps, G. Bouhadir, W. Gu, M. Mercy, C. Chen, B. M. Foxman, L. Maron, O. V. Ozerov and D. Bourissou, *Angew. Chem., Int. Ed.*, 2008, **47**, 1481–1484.
- 29 H. W. Harman and J. C. Peters, *J. Am. Chem. Soc.*, 2012, **134**, 5080–5082.
- 30 W. H. Harman, T.-P. Lin and J. C. Peters, *Angew. Chem., Int. Ed.*, 2014, **53**, 1081–1086.
- 31 (a) G. Zeng and S. Sakaki, *Inorg. Chem.*, 2013, **52**, 2844–2853; (b) Y. Li, C. Hou, J. Jiang, Z. Zhang, C. Zhao, A. J. Page and Z. Ke, *ACS Catal.*, 2016, **6**, 1655–1662.
- 32 S. N. MacMillan, H. W. Harman and J. C. Peters, *Chem. Sci.*, 2013, **5**, 590–597.
- 33 M.-E. Moret and J. C. Peters, *Angew. Chem., Int. Ed.*, 2011, **50**, 2063–2067.
- 34 J. S. Anderson, J. Rittle and J. C. Peters, *Nature*, 2013, **501**, 84.
- 35 T. M. Buscagan, P. H. Oyala and J. C. Peters, *Angew. Chem., Int. Ed.*, 2017, **56**, 6921–6926.



36 (a) M. Moret and J. C. Peters, *J. Am. Chem. Soc.*, 2011, **133**, 18118–18121; (b) J. S. Anderson, M.-E. Moret and J. C. Peters, *J. Am. Chem. Soc.*, 2013, **135**, 534–537.

37 H. Fong, M.-E. Moret, Y. Lee and J. C. Peters, *Organometallics*, 2013, **32**, 3053–3062.

38 H. Kameo, J. Yamamoto, A. Asada, H. Nakazawa, H. Matsuzaka and D. Bourissou, *Angew. Chem., Int. Ed.*, 2019, **58**, 18783–18787.

39 F. Inagaki, C. Matsumoto, Y. Okada, N. Maruyama and C. Mukai, *Angew. Chem., Int. Ed.*, 2015, **54**, 818–822.

40 (a) F. Inagaki, K. Nakazawa, K. Maeda, T. Koseki and C. Mukai, *Organometallics*, 2017, **36**, 3005–3008; (b) C. Matsumoto, M. Yamada, X. Dong, C. Mukai and F. Inagaki, *Chem. Lett.*, 2018, **47**, 1321–1323; (c) F. Inagaki, K. Maeda, K. Nakazawa and C. Mukai, *Eur. J. Org. Chem.*, 2018, 2972–2976.

41 Y. Segawa, M. Yamashita and K. Nozaki, *J. Am. Chem. Soc.*, 2009, **131**, 9201–9203.

42 (a) H. Ogawa and M. Yamashita, *Dalton Trans.*, 2012, **42**, 625–629; (b) T. Miyada, E. Kwan and M. Yamashita, *Organometallics*, 2014, **33**, 6760–6770; (c) H. Ogawa and M. Yamashita, *Chem. Lett.*, 2014, **43**, 664–666; (d) K. Tanoue and M. Yamashita, *Organometallics*, 2015, **34**, 4011–4017; (e) E. Kwan, H. Ogawa and M. Yamashita, *ChemCatChem*, 2017, **9**, 2457–2462.

43 E. Kwan, Y. Kawai, S. Kamakura and M. Yamashita, *Dalton Trans.*, 2016, **45**, 15931–15941.

44 P. Ríos, N. Curado, J. López-Serrano and A. Rodríguez, *Chem. Commun.*, 2015, **52**, 2114–2117.

45 Y. Ding, Q.-Q. Ma, J. Kang, J. Zhang, S. Li and X. Chen, *Dalton Trans.*, 2019, **48**, 17633–17643.

46 T.-P. Lin and J. C. Peters, *J. Am. Chem. Soc.*, 2013, **135**, 15310–15313.

47 T.-P. Lin and J. C. Peters, *J. Am. Chem. Soc.*, 2014, **136**, 13672–13683.

48 (a) W.-C. Shih, W. Gu, M. C. MacInnis, S. D. Timpa, N. Bhuvanesh, J. Zhou and O. V. Ozerov, *J. Am. Chem. Soc.*, 2016, **138**, 2086–2089; (b) W.-C. Shih, W. Gu, M. C. MacInnis, D. E. Herbert and O. V. Ozerov, *Organometallics*, 2017, **36**, 1718–1726; (c) W.-C. Shih and O. V. Ozerov, *J. Am. Chem. Soc.*, 2017, **139**, 17297–17300.

49 W.-C. Shih and O. V. Ozerov, *Organometallics*, 2016, **36**, 228–233.

50 (a) L. Vondung, N. Frank, M. Fritz, L. Alig and R. Langer, *Angew. Chem., Int. Ed.*, 2016, **55**, 14450–14454; (b) L. Vondung, L. Alig, M. Ballmann and R. Langer, *Chem.–Eur. J.*, 2018, **24**, 12346–12353.

51 (a) M. Grätz, A. Bäcker, L. Vondung, L. Maser, A. Reincke and R. Langer, *Chem. Commun.*, 2017, **53**, 7230–7233; (b) L. Maser, C. Schneider, L. Alig and R. Langer, *Inorganics*, 2019, **7**, 61.

52 A. Bäcker, Y. Li, M. Fritz, M. Grätz, Z. Ke and R. Langer, *ACS Catal.*, 2019, **9**, 7300–7309.

53 Catalytic hydroboration and hydrosilylation reactions utilizing  $[\text{Fe}(\text{CH}_3\text{CN})_6][\text{Fe}(\text{CO})_4(\text{InCl}_3)_2]$  were reported, where an Fe–In bond is proposed to remain intact during the catalysis without a multidentate support. See: (a) M. Ito, M. Itazaki and H. Nakazawa, *ChemCatChem*, 2016, **8**, 3323–3325; (b) M. Ito, M. Itazaki and H. Nakazawa, *Inorg. Chem.*, 2017, **56**, 13709–13714.

54 (a) P. Rudd, S. Liu, L. Gagliardi, V. G. Young and C. C. Lu, *J. Am. Chem. Soc.*, 2011, **133**, 20724–20727; (b) P. A. Rudd, N. Planas, E. Bill, L. Gagliardi and C. C. Lu, *Eur. J. Inorg. Chem.*, 2013, 3898–3906; (c) J. T. Moore, N. E. Smith and C. C. Lu, *Dalton Trans.*, 2017, **46**, 5689–5701; (d) M. V. Vollmer, J. Xie and C. C. Lu, *J. Am. Chem. Soc.*, 2017, **139**, 6570–6573; (e) M. V. Vollmer, J. Xie, R. C. Cammarota, V. G. Young, E. Bill, L. Gagliardi and C. C. Lu, *Angew. Chem., Int. Ed.*, 2018, **57**, 7815–7819; (f) M. V. Vollmer, R. C. Cammarota and C. C. Lu, *Eur. J. Inorg. Chem.*, 2019, 2140–2145; (g) R. C. Cammarota, L. J. Clouston and C. C. Lu, *Coord. Chem. Rev.*, 2017, **334**, 100–111.

55 (a) R. C. Cammarota and C. C. Lu, *J. Am. Chem. Soc.*, 2015, **137**, 12486–12489; (b) R. C. Cammarota, M. V. Vollmer, J. Xie, J. Ye, J. C. Linehan, S. A. Burgess, A. M. Appel, L. Gagliardi and C. C. Lu, *J. Am. Chem. Soc.*, 2017, **139**, 14244–14250; (c) J. Ye, R. C. Cammarota, J. Xie, M. V. Vollmer, D. G. Truhlar, C. J. Cramer, C. C. Lu and L. Gagliardi, *ACS Catal.*, 2018, **8**, 4955–4968.

56 Lu reported the preparation of a metal–organic framework consisting of well-defined Rh–Ga catalytic sites and its catalysis for a semihydrogenation reaction of alkynes to give *trans*-alkenes. See: (a) S. P. Desai, J. Ye, J. Zheng, M. S. Ferrandon, T. E. Webber, A. E. Platero-Prats, J. Duan, P. Garcia-Holley, D. M. Camaioni, K. W. Chapman, M. Delferro, O. K. Farha, J. L. Fulton, L. Gagliardi, J. A. Lercher, R. L. Penn, A. Stein and C. C. Lu, *J. Am. Chem. Soc.*, 2018, **140**, 15309–15318; (b) S. P. Desai, J. Ye, T. Islamoglu, O. K. Farha and C. C. Lu, *Organometallics*, 2019, **38**, 3466–3473.

57 M. V. Vollmer, J. Ye, J. C. Linehan, B. J. Graziano, A. Preston, E. S. Wiedner and C. C. Lu, *ACS Catal.*, 2020, **10**, 2459–2470.

58 J. T. Moore and C. C. Lu, *J. Am. Chem. Soc.*, 2020, **142**, 11641–11646.

59 (a) J. Takaya and N. Iwasawa, *J. Am. Chem. Soc.*, 2017, **139**, 6074–6077; (b) N. Saito, J. Takaya and N. Iwasawa, *Angew. Chem., Int. Ed.*, 2019, **58**, 9998–10002; (c) J. Takaya, M. Hoshino, K. Ueki, N. Saito and N. Iwasawa, *Dalton Trans.*, 2019, **48**, 14604–14610.

60 (a) N. Hara, T. Saito, K. Semba, N. Kuriakose, H. Zheng, S. Sakaki and Y. Nakao, *J. Am. Chem. Soc.*, 2018, **140**, 7070–7073; (b) N. Kuriakose, J.-J. Zheng, T. Saito, N. Hara, Y. Nakao and S. Sakaki, *Inorg. Chem.*, 2019, **58**, 4894–4906; (c) T. Saito, N. Hara and Y. Nakao, *Chem. Lett.*, 2017, **46**, 1247–1249.

61 I. Fujii, K. Semba, Q.-Z. Li, S. Sakaki and Y. Nakao, *J. Am. Chem. Soc.*, 2020, **142**, 11647–11652.

62 S. Morisako, S. Watanabe, S. Ikemoto, S. Muratsugu, M. Tada and M. Yamashita, *Angew. Chem., Int. Ed.*, 2019, **58**, 15031–15035.

63 R. Yamada, N. Iwasawa and J. Takaya, *Angew. Chem., Int. Ed.*, 2019, **58**, 17251–17254.



64 (a) J. Y. Corey and J. Braddock-Wilking, *Chem. Rev.*, 1999, **99**, 175–292; (b) J. Y. Corey, *Chem. Rev.*, 2011, **111**, 863–1071; (c) J. Y. Corey, *Chem. Rev.*, 2016, **116**, 11291–11435.

65 For selected examples; see: (a) D. E. Hendriksen, A. A. Oswald, G. B. Ansell, S. Leta and R. V. Kastrup, *Organometallics*, 1989, **8**, 1153–1157; (b) P. Sangtrirutnugul and T. D. Tilley, *Organometallics*, 2007, **26**, 5557–5568; (c) M. C. MacInnis, D. F. MacLean, R. J. Lundgren, R. McDonald and L. Turculet, *Organometallics*, 2007, **26**, 6522–6525; (d) Y.-H. Li, Y. Zhang and X.-H. Ding, *Inorg. Chem. Commun.*, 2011, **14**, 1306–1310; (e) H.-W. Suh, L. M. Guard and N. Hazari, *Chem. Sci.*, 2014, **5**, 3859–3872; (f) H.-W. Suh, L. M. Guard and N. Hazari, *Polyhedron*, 2014, **84**, 37–43; (g) T. Komuro, T. Arai, K. Kikuchi and H. Tobita, *Organometallics*, 2015, **34**, 1211–1217; (h) Z. Xiong, X. Li, S. Zhang, Y. Shi and H. Sun, *Organometallics*, 2016, **35**, 357–363; (i) B. A. Connor, J. Rittle, D. VanderVelde and J. C. Peters, *Organometallics*, 2016, **35**, 686–690; (j) L. J. Murphy, H. Hollenhorst, R. McDonald, M. Ferguson, M. D. Lumsden and L. Turculet, *Organometallics*, 2017, **36**, 3709–03720; (k) L. J. Murphy, A. J. Ruddy, R. McDonald, M. J. Ferguson and L. Turculet, *Eur. J. Inorg. Chem.*, 2018, 4481–4493; (l) P. Zhang, X. Li, X. Qi, H. Sun, O. Fuhr and D. Fenske, *RSC Adv.*, 2018, **8**, 14092–14099; (m) T. Komuro, T. Osawa, R. Suzuki, D. Mochizuki, H. Higashi and H. Tobita, *Chem. Commun.*, 2019, **55**, 957–960.

66 S. J. Mitton and L. Turculet, *Chem.-Eur. J.*, 2012, **18**, 25258–25263.

67 L. J. Murphy, M. J. Ferguson, R. McDonald, M. D. Lumsden and L. Turculet, *Organometallics*, 2018, **37**, 4814–4826.

68 (a) J. Takaya and N. Iwasawa, *J. Am. Chem. Soc.*, 2008, **130**, 15254–15255; (b) J. Takaya, K. Sasano and N. Iwasawa, *Org. Lett.*, 2011, **13**, 1698–1701.

69 J. Takaya and N. Iwasawa, *Organometallics*, 2009, **28**, 6636–6638.

70 (a) C. Zhu, J. Takaya and N. Iwasawa, *Org. Lett.*, 2015, **17**, 1814–1817; (b) J. Takaya, K. Miyama, C. Zhu and N. Iwasawa, *Chem. Commun.*, 2017, **53**, 3982–3985.

71 (a) J. Takaya and N. Iwasawa, *Chem.-Eur. J.*, 2014, **20**, 11812–11819; (b) J. Takaya and N. Iwasawa, *Dalton Trans.*, 2011, **40**, 8814–8821.

72 J. Takaya and N. Iwasawa, *Eur. J. Inorg. Chem.*, 2018, 5012–5018.

73 (a) J. Takaya, N. Kirai and N. Iwasawa, *J. Am. Chem. Soc.*, 2011, **133**, 12980–12983; (b) N. Kirai, S. Iguchi, T. Ito, J. Takaya and N. Iwasawa, *Bull. Chem. Soc. Jpn.*, 2013, **86**, 784–799.

74 (a) N. Kirai, J. Takaya and N. Iwasawa, *J. Am. Chem. Soc.*, 2013, **135**, 2493–2496; (b) J. Takaya, N. Kirai and N. Iwasawa, *Organometallics*, 2014, **33**, 1499–1502.

75 J. Takaya, S. Ito, H. Nomoto, N. Saito, N. Kirai and N. Iwasawa, *Chem. Commun.*, 2015, **51**, 17662–17665.

76 A related Pt-catalyzed  $sp^2$ C–H borylation at sterically congested positions was reported at almost the same time. See: T. Furukawa, M. Tobisu and N. Chatani, *J. Am. Chem. Soc.*, 2015, **137**, 12211–12214.

77 (a) H. Tobita, N. Yamahira, K. Ohta, T. Komuro and M. Okazaki, *Pure Appl. Chem.*, 2008, **80**, 1155–1160; (b) T. Komuro, T. Kitano, N. Yamahira, K. Ohta, S. Okawara, N. Mager, M. Okazaki and H. Tobita, *Organometallics*, 2016, **35**, 1209–1217.

78 T. Kitano, T. Komuro, R. Ono and H. Tobita, *Organometallics*, 2017, **36**, 2710–2713.

79 (a) A. Brück, D. Gallego, W. Wang, E. Irran, M. Driess and J. F. Hartwig, *Angew. Chem. Int. Ed.*, 2012, **51**, 11478–11482; (b) D. Gallego, A. Brück, E. Irran, F. Meier, M. Kaupp, M. Driess and J. F. Hartwig, *J. Am. Chem. Soc.*, 2013, **135**, 15617–15626.

80 (a) W. Levason and G. Reid, *Coord. Chem. Rev.*, 2006, **250**, 2565–2594; (b) H. Braunschweig, P. Cogswell and K. Schwab, *Coord. Chem. Rev.*, 2011, **255**, 101–117; (c) S. Roggan and C. Limberg, *Inorg. Chim. Acta*, 2006, **359**, 4698–4722.

81 S. L. Benjamin and G. Reid, *Coord. Chem. Rev.*, 2015, **297–298**, 168–180.

82 (a) T. Lin, C. R. Wade, L. M. Pérez and F. P. Gabbaï, *Angew. Chem. Int. Ed.*, 2010, **49**, 6357–6360; (b) C. R. Wade, T.-P. Lin, R. C. Nelson, E. A. Mader, J. T. Miller and F. P. Gabbaï, *J. Am. Chem. Soc.*, 2011, **133**, 8948–8955; (c) T.-P. Lin, R. C. Nelson, T. Wu, J. T. Miller and F. P. Gabbaï, *Chem. Sci.*, 2011, **3**, 1128–1136; (d) C. R. Wade, I. Ke and F. P. Gabbaï, *Angew. Chem. Int. Ed.*, 2012, **51**, 478–481; (e) I.-S. Ke and F. P. Gabbaï, *Inorg. Chem.*, 2013, **52**, 7145–7151; (f) I. Ke, J. S. Jones and F. P. Gabbaï, *Angew. Chem. Int. Ed.*, 2014, **53**, 2633–2637; (g) J. S. Jones, C. R. Wade and F. P. Gabbaï, *Angew. Chem. Int. Ed.*, 2014, **53**, 8876–8879; (h) H. Yang and F. P. Gabbaï, *J. Am. Chem. Soc.*, 2014, **136**, 10866–10869; (i) J. S. Jones, C. R. Wade and F. P. Gabbaï, *Organometallics*, 2015, **34**, 2647–2654; (j) S. Sen, I.-S. Ke and F. P. Gabbaï, *Inorg. Chem.*, 2016, **55**, 9162–9172; (k) S. J. Jones, C. R. Wade, M. Yang and F. P. Gabbaï, *Dalton Trans.*, 2017, **46**, 5598–5604; (l) S. Sahu and F. P. Gabbaï, *J. Am. Chem. Soc.*, 2017, **139**, 5035–5038.

83 (a) H. Yang and F. P. Gabbaï, *J. Am. Chem. Soc.*, 2015, **137**, 13425–13432; (b) S. Sen, I.-S. Ke and F. P. Gabbaï, *Organometallics*, 2017, **36**, 4224–4230.

84 D. You, H. Yang, S. Sen and F. P. Gabbaï, *J. Am. Chem. Soc.*, 2018, **140**, 9644–9651.

85 Y. Lo and F. P. Gabbaï, *Angew. Chem. Int. Ed.*, 2019, **58**, 10194–10197.

86 (a) D. You and F. P. Gabbaï, *J. Am. Chem. Soc.*, 2017, **139**, 6843–6846; (b) D. You, J. E. Smith, S. Sen and F. P. Gabbaï, *Organometallics*, DOI: 10.1021/acs.organomet.0c00193.

87 (a) T.-P. Lin, I.-S. Ke and F. P. Gabbaï, *Angew. Chem. Int. Ed.*, 2012, **51**, 4985–4988; (b) I.-S. Ke and F. P. Gabbaï, *Aust. J. Chem.*, 2013, **66**, 1281.

88 (a) C. Tschersich, C. Limberg, S. Roggan, C. Herwig, N. Ernsting, S. Kovalenko and S. Mebs, *Angew. Chem. Int. Ed.*, 2012, **51**, 4989–4992; (b) C. Tschersich, B. Braun, C. Herwig and C. Limberg, *J. Organomet. Chem.*, 2015, **784**, 62–68.

89 (a) K. Materne, B. Braun-Cula, C. Herwig, N. Frank and C. Limberg, *Chem.-Eur. J.*, 2017, **23**, 11797–11801; (b)



K. Materne, S. Hoof, N. Frank, C. Herwig and C. Limberg, *Organometallics*, 2017, **36**, 4891–4895.

90 (a) E. V. Dikarev, T. G. Gray and B. Li, *Angew. Chem., Int. Ed.*, 2005, **44**, 1721–1724; (b) E. V. Dikarev, B. Li and H. Zhang, *J. Am. Chem. Soc.*, 2006, **128**, 2814–2815.

91 J. Hansen, B. Li, E. Dikarev, J. Autschbach and H. M. Davies, *J. Org. Chem.*, 2009, **74**, 6564–6571.

92 L. R. Collins, M. van Gastel, F. Neese and A. Fürstner, *J. Am. Chem. Soc.*, 2018, **140**, 13042–13055.

93 L. R. Collins, S. Auris, R. Goddard and A. Fürstner, *Angew. Chem., Int. Ed.*, 2019, **58**, 3557–3561.

